Semi-Annual Status Report

for the period

September 15, 1975 through February 15, 1976

Submitted Under

NASA Grant NSG 1249

entitled

Flight Test of a Stall Sensor and Evaluation of its Application to an Aircraft Stall Deterrent System Using the NASA LRC General Aviation Simulator

by

Dr. George Bennett and Dr. John K. Owens

Mississippi State University
Aerophysics and Aerospace Engineering
Mississippi State, Mississippi 39762

March 5, 1976

(NASA-CR-146324) FIIGHT TEST OF A STALL SENSOR AND EVALUATICN OF ITS APPLICATION TO AN AIRCRAFT STALL DETERRENT SYSTEM USING THE NASA LRC GENERAL AVIATION SIMULATOR Semiannual Status (Mississippi State Univ., G3/06

N76-18115

HC $4.00

Unclas

20456

TABLE OF CONTENTS

List of Symbols

$\bar{c}$	airplane mean aerodynamic chord, ft.
C_{L_α}	airplane lift slope, 1/rad
$C_m(\alpha)$	airplane arbitrary pitching moment curve
C_{m_o}	zero lift pitching moment
C_{m_q}	pitch damping, sec/rad
C_{m_α}	linear moment derivative, 1/rad
C_{m_δ}	elevator control derivative, 1/rad
I_y	airplane pitch moment of inertia, slug ft^2
k_s	angle of attack error gain, rad/volt
k_r	pitch rate gain, rad/volt/sec
M	aerodynamic moment = $C_m \frac{1}{2} \rho V^2 S_w \bar{c}$, ft lbs
S_w	airplane wing area, ft^2
t_s	first order time constant for linear servo, sec
V	airplane speed, ft/sec
V_s	sensor output, volts
V_{s_1}	sensor output at control point,
V_{s_2}	sensor output for control saturation
W	airplane weight, lbs
α	airplane angle of attack, rad
α_1	angle of attack for control onset, rad

δ_e	elevator deflection, rad
$\delta_{e_{trim}}$	trim elevator deflection, rad
δ_s	stall deterrent servo elevator increment, rad
$\Delta\delta_{e_p}$	pilot elevator command, rad

List of Illustrations

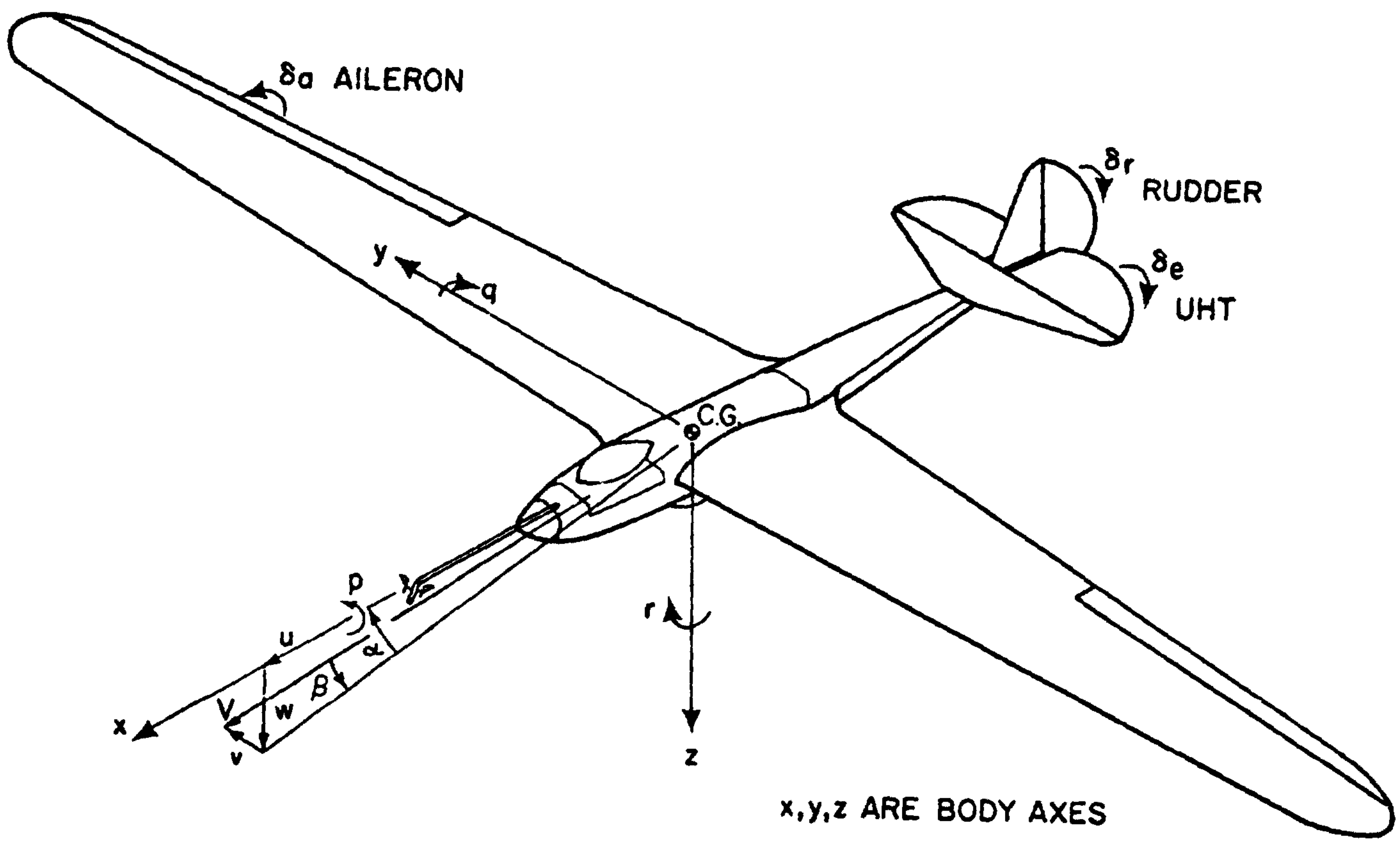
δa AILERON
δr RUDDER
δe
UHT
y
q
C.G.
p
u
α
β
V
w
v
x
r
z
x,y,z ARE BODY AXES

AXIS SYSTEM

Acknowledgements

The authors wish to thank Dr. Willie T. McDaniel, Director of the Engineering and Industrial Research Station, for providing funds for a research assistantship on the Stall Deterrent program. The authors also wish to thank Dr. Randall Harris, and other members of the Flight Vehicles Research Branch of FDCD for their assistance in the performance of the simulation portion of this research and for their suggestions and timely criticism of the Flight test activity. Finally, the authors wish to thank Mr. Michael L. King, graduate student, for his unceasing efforts on the Stall Deterrent research program.

Summary

The major tasks accomplished during the first half of the grant period were completion of aircraft instrumentation system, execution of 17 test flights, initial development of the acoustic sensor signal conditioning unit, and development of stall deterrent system simulation computer programs. The analog data reduction system has allowed very rapid analysis of flight test data and simplified the development of the sensor signal conditioning circuits.

A series of flight maneuvers have been developed to cover the range of flight conditions and to define the repeatability and hysteresis of the sensors. Initial flights have been made with two sensors at the $\pm$68% span and 60% and 70% chord stations.

The primary effort in simulation program development has been to modify the LRC General Aviation Simulator (GAS) Fortran programs to allow execution on the MSU UNIVAC 1106. A simple model of the sensor-servo stall deterrent system has been developed. Initial testing of this model was made on the LRC GAS January 28 and 29, 1976. A one degree of freedom model of pitch dynamics of the airplane and stall deterrent system has been developed to make initial estimates of the control system gains. A position error plus rate damping control algorithm has been found to have acceptable characteristics.

Introduction

The objectives of this study are to determine the suitability of the acoustic velocity fluctuation sensor for the detection of wing stall and the pilot acceptibility of an active pitch control intervention system for stall deterrence. The acoustic sensor is attractive because of its rugged construction and low cost. This study is directed toward determining the sensor output characteristics over a range of power settings, flap positions, and sideslip angles normally encountered in high angle of attack flight.

The concept of active intervention during stall must be examined carefully to determine the interaction between the aircraft, control system and pilot in a high stress environment. The Langley Research General Aviation Simulator is ideally suited for this study because of the computational power, the realistic visual scene, and the complete cockpit which includes motion cues.

The sections which follow describe the work completed at this point. The flight testing is currently progressing very well. The Cessna 319 (Figs. 1 & 2) has proved to be a very good vehicle for this research. The ease of access to the wing structure and the cabin area plus the large payload capability has made the testing pleasant. Table 1 shows the program schedule and the current status of the various tasks. The flight testing is scheduled to be completed by April 15, subject to the availability of the Aztec aircraft. The extensive modifications to the Aztec for cooling studies have taken much longer than anticipated.

The simulator evaluation session has been broken up into two parts to avoid a long absence from the classroom. Also we have found that checkout of the simulator for high angle of attack flight is very slow and tedious

A very brief checkout of the stall deterrent system was conducted January 28 and 29, 1976. A one week session is scheduled for April 10 through April 16, 1976. The final session is to be scheduled for May 24 through May 28, 1976.

Sensor Design

The acoustic probes used in this study are shown in Figs. 3 and 4. The probes were constructed of Ward's Bio-Plastic liquid casting plastic to allow easy inspection of the orifice cavity. It has been found that several holes can be drilled in each probe and the appropriate hole exposed during each flight. A Shure microphone is used for these studies. The cost is low and the response very adequate. The slot orifice was test flown, however, the acoustic signal did not appear to be suitable for high angle of attack control. In Fig. 2, the test locations for the probes are shown. The flights up to this point have been at the 68% span station and 60% and 70% chord stations.

Flight Test Instrumentation

The flight test instrumentation system installed in the 319 is shown in Fig. 5 and a complete schematic is shown in Fig. 6. A signal conditioning box contains the signal conditioning amplifiers and their associated power supplies. The amplifier gains are adjusted such that the outputs range between ± 1.3 volts for full scale input of the parameters. This value of amplifier output is set to be compatible with the Lockheed analog tape recorder. A set of potentiometer sensors measure angle of attack, yaw angle, and elevator deflection angle. The potentiometers are energized from a five volt regulated power supply. This power supply has been extensively tested and it has regulation better than 0.5% over the 0 degrees C to 50 degrees C temperature region of operation. The angle of attack and yaw sensors have given problems due to the flutter of the probe during high speed flight. The potentiometers used in the probe are very small and possibly are not rugged enough for this application. A Northam 0.15 psid variable reluctance pressure transducer is used with a Pace CD-17 signal conditioning unit to measure airspeed. The pressure transducer and signal conditioning units are mounted in the signal conditioning box where the temperature is held constant at approximately 25 degrees C. An inverter that converts aircraft 24V to 115VAC at 400 Hz is used to power the entire system. A Lockheed Model 417 analog tape recorder is used to record all data. The recorder has a voice track that is used to keep track of the operation and mark the various events that occur during a flight. A digital voltmeter is included in the instrumentation system so that a constant check can be kept on the excitation to the potentiometers and other pertinent parameters. Two magnetic microphones are used as the stall sensors. These microphones are mounted in the wings of the aircraft. The output of the microphones is conditioned in the signal conditioning box.

Data Reduction

The analog computer was chosen for the data reduction because of the few channels being recorded and the high frequency acoustic signals. Fig. 8 shows the installation of the equipment and Fig. 9 is a complete schematic. Calibration of the α,β and δ_e position sensors showed that a linear fit was appropriate for α and δ_e, and a function generator was necessary for the β output. The pressure transducer was found to be very linear, thus a square root device was appropriate.

Calibration voltages were recorded at the beginning and end of each flight to check the record/playback accuracy of the tape deck and to allow an entire system checkout. A Hewlett Packard Data Logger was used to scan both input and output of the analog system during the calibration voltage inputs to give a hard copy record. It has been found that both the airborne instrumentation package and the data reduction system are very stable and require little attention.

The data reduction is done in real time, thus the time required to process each flight is of order 2 hours. This short turnaround allows analysis of the flight test data within one day of the flight.

Acoustic Signal Processing

The extent of the signal processing to date has been to amplify the raw sensor signal to a level compatible with the Lockheed Model 417 Analog tape recorder and to further condition the data by means of a full wave rectifier with an averaging filter. This rectifier-filter has been used to produce an output signal that will be adequate for control. Fig. 10 of this progress report shows the full wave rectifier and averaging circuit that is in current use.

No attempt has been made to evaluate discrimination levels because the sensor position on the wing has not yet been fixed. The height of the sensor inlet above the wing is also in question at this time. The processing of additional flights of data will be required before this problem of sensor location and height can be fully resolved. The data to date indicates that a position of 60% chord and a height of 1.25" is acceptable.

A minor problem (though a pleasant one) that has arisen is the fact that at most of the locations tested, the sensor shows an early turn on if it is yawed into the rear position. If an assessment of the flight regime indicates that this is a problem, it is felt that by summing the output of the two sensors (one on each wing) a reliable and uniform signal can be produced. Several signal summing possibilities exist and will be considered during the latter half of the program. These possibilities will be investigated with reliability of the system as a primary goal.

Flight Test Program, Maneuvers and Discussion of Initial Results

The objective of the flight test program is to determine the characteristics of the sensor output as a function of airplane angle of attack, sideslip angle, power setting, flap setting, sensor position, sensor orifice height and orifice shape. Table 2 shows the set of maneuvers which have been developed to cover the range of stall approaches which are of interest. It was found that the hysteresis and repeatability of the sensor output could be investigated by making three angle of attack variations within each maneuver. First a slow airspeed bleed rate to the onset of significant buffet, then the airspeed is allowed to slowly increase to a fully unstalled condition, then a faster bleed rate is applied to buffet and recovery. Finally the aircraft is taken to a fully stalled condition with full elevator deflection. Usually a stall departure is encountered with this final maneuver and a spin entry is made. The 319 will spin, but recovery is rapid when proper control inputs are given.

Table 3 shows the flights completed at this time. After initial problems with temperature drift of the potentiometer sensor power supply, the system has proved to be very reliable. Flt. 10 was the first flight that yielded acceptable data. The results of this flight will be discussed later in this section.

Flights 3 through 6 were made to establish position error of the pitot-static probe and the wing upwash correction for the α probe. It was found that the position error was less than the uncertainty in the airspeed indicator calibration. A good vertical gyro was not available for the calibration of the upwash correction for the α probe, and an inclinometer was used instead. The upwash correction was not discernible from the data, thus no correction was made.

The stall pattern on the 319 wing was photographed using a 16 mm movie camera. The Cessna 150 was used as the photographic platform. A review of the movie film shows that we must reduce the film exposure, increase the tuft size, and reduce the area of coverage by the camera to obtain better resolution of the stall pattern. The photographic flight will be repeated shortly.

The following discussion illustrates the data that is obtained during the flight test program. The Visicorder output has been traced for the particular case shown due to poor contrast of the original data. The α-β probe was reworked following the data reduction, preventing reprocessing the data. The time constant on the averaging filter was 1 second. Subsequent data reduction has used a 0.2 second time constant. The sensor configuration was a 1 1/4" height hole orifice on the left wing and a 1" height hole orifice on the right wing. The sensor positions were at 70% chord and 68% span. See Fig. 2 for the sensor position relative to the flaps and ailero

Figs. 11 through 15 show the data obtained for the zero flap, trim at 70 mph configuration for 0 and ±10 degree sideslip angles. The general result is that the 1" height orifice is too close to the wing at the 70% chord position and picks up the boundary layer large scale fluctuations at very low angles of attack. Fig. 14 shows the variation of sensor processed output versus α for the 1" orifice height. This signal is not suitable for a control function and will not be considered further.

The 1 1/4" height orifice in Fig. 11 shows the gradual onset of stall with sensor output peaking before α stall is reached. The long time constant of the filter causes the slow response of sensor processed output during the stall recovery. Fig. 12 shows the sensor response for the 10 degree sideslip angle. This yaw condition places the right wing forward and the boundary layer buildup is small. However, Fig. 13 shows the effect of the thickened layer on the trailing wing. The sensor acoustic signal is initiated at a lower angle of attack and the amplitude is doubled. The processed sensor response versus angle of attack is shown in Fig. 15 for 0 and ± 10 degree sideslip angle. Note that the peak sensor output occurs at an angle of attack less than the stall angle. Both of these characteristics of the processed signal must be modified for a stall deterrent application.

Figs. 16 through 20 show the effect of full flap upon the sensor outputs for Flight 10. Analysis of the processed sensor output versus angle of attack plots on Fig. 19 shows that the response is similar to the flaps up configuraion in output voltage levels and angles of attack for onset and maximum output. Thus for the configuration chosen we can see little flap effects.

Table 3 shows a log of the sensor configurations and positions tested up to this time. No further flight testing is to be conducted until a thorough analysis is made of all of the data obtained through Fl ght 17.

Stall Deterrent System Studies

The modification of the LRC General Aviation Simulator (GAS) to be compatible with the MSU UNIVAC 1106 has proved to be more difficult than anticipated. Also, a significant effort was made to develop an editing capability which would allow the generation of an extensive definition of symbols and simplify the modification of the programs. This area is to receive more attention during the remainder of the contract period.

In view of these difficulties with the more complex simulation, a simple one degree of freedom simulation program was developed to allow the initial shaping of the stall deterrent control system for use on the LRC GAS.

For a one DOF system we can equate α and body attitude, θ. Thus

$$I_y\ddot{\theta} = \Sigma M = I_y\ddot{\alpha} \tag{1}$$

Assume moments about c.g. thus only aerodynamic moments will be considered. Then we can write

$$I_y\ddot{\alpha} = \left[C_m(\alpha) + C_{m_o} + C_{m_\alpha} + C_{m_\delta}\delta_e + C_{m_q}\frac{\bar{c}}{2V}{}^{2}\right]\frac{1}{2}\rho V^2\bar{c}S_w \tag{2}$$

Define

$$A = \frac{1/2\rho V^2\bar{c}S_w}{I_y} \tag{3}$$

Then we can write (2) as two first order differential equations if $\dot{\alpha} \equiv q$.

$$\dot{\alpha} \equiv q \tag{4}$$

$$\dot{q} = \left[C_{m_o} + C_{m_\alpha}\alpha + C_m(\alpha) + C_{m_\delta}\delta_e + C_{m_q}\frac{\bar{c}}{2V}{}^{2}\right]A \tag{5}$$

First we must "trim up" the aircraft for static equilibrium. For

trim

$$\delta_{e_{trim}} = \left[-C_{m_o} + C_{m_\alpha}\alpha + C_m(\alpha)\right] / C_{m_\delta} \tag{6}$$

where we assume L = W, thus

$$\alpha = \frac{W/S_w}{C_{L_\alpha} 1/2\rho V^2} \tag{7}$$

A Runga-Kutta integration routine was used to integrate these equations over time. Of interest is the response of the system to pilot and stall deterrent system inputs to elevator deflection.

The stall deterrent system is designed to limit angle of attack to avoid wing stall. For this system, a linear servo is placed between the pilot and the elevator so that the airplane elevator deflection is the sum of the pilot and servo inputs. For this model we assume the pilot input is a perturbation from trim, thus

$$\delta_e = \delta_{e_{trim}} + \Delta\delta_{e_p}(t) + \delta_s \tag{8}$$

The pilot control inputs were made via a table lookup time history, thus arbitrary control motions are possible. The stall deterrent system consists of an angle of attack sensor, a control logic unit, and a linear servo. The acoustic sensor has a nonlinear response to angle of attack. For this simulation study, a simplified curve shown in Fig. 21 has been assumed. The system is designed to limit α to 12.5 degrees. Two control laws have been studied. A position command system as shown in Fig. 22 has been defined.

For $V_s < V_{s_1}$ i.e. $\alpha < \alpha_1$

$$\delta_s = 0 \tag{9}$$

For $V_{s_1} < V_s < V_{s_2}$

$$\delta_s = k_v(V_s - V_{s_1}) + k_r \frac{dV_s}{dt}$$

The linear servo is assumed to have a first order response with a 0.2 sec. time constant. No system hysteresis is assumed.

A similar control scheme using rate command is being explored, but poor control has been accomplished for high pilot deflection rates.

The results of an analysis of Cessna 172 response is shown in Figs. 23 and 24. The following parameters were assumed.

$W = 2000$ lbs.	$C_{L_\alpha} = 4.89$
$I_y = 1244$ slug ft^2	$C_m(\alpha) = 0.0$
$S_w = 174$ ft	$C_{m_\alpha} = 0.98$
$\rho = 0.0024$ slug/ft^3	$C_{m_o} = 0.0$
$V = 130$ ft/sec	$C_{m_\delta} = 1.72$
$\bar{c} = 4.8$ ft	$C_{m_q} = -10.0$
$t_s = 0.2$ sec	$k_s = .175$ rad/volt
	$k_r = .1$ rad/volt/sec

Fig. 23 shows the system response to a 20 degree per second, 20 degree ramp pilot input. Note the system exhibits little overshoot and trims at $\alpha = 15$ degrees. It has been found that if very high pilot command pitch rates are input, the aircraft will pass through the sensor control region too quickly for angle of attack limiting to take place. We are currently investigating the maximum pitch rates possible in the 319 to support this work.

Fig. 24 shows the system response to a pilot spike input. Note the long time required to damp after return to trim is due to no control inputs and only aircraft damping active.

The next step is to continue these simulation experiments using the GAS programs in a three degree of freedom mode.

Table 1

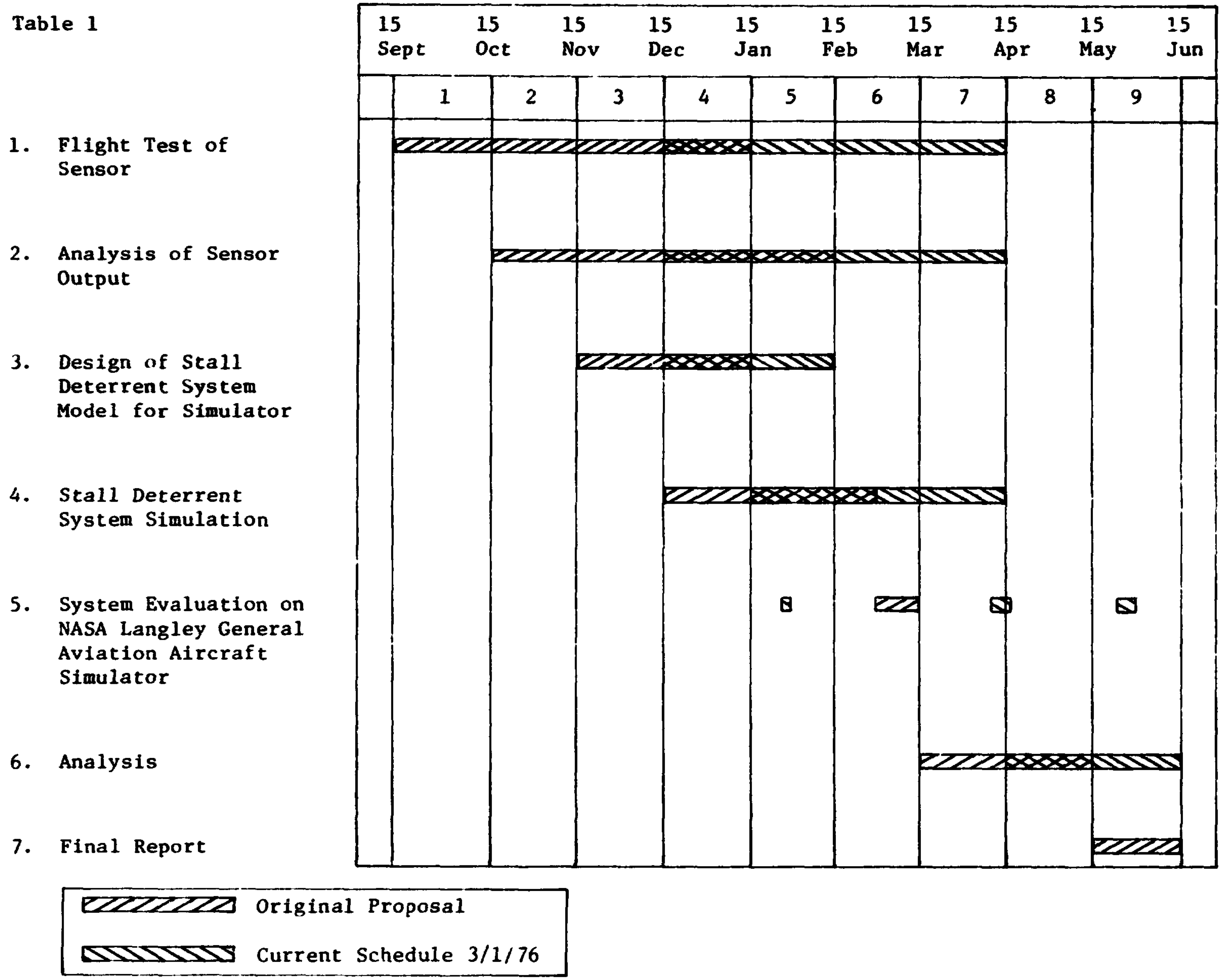
15 Sept
15 Oct
15 Nov
15 Dec
15 Jan
15 Feb
15 Mar
15 Apr
15 May
15 Jun
1
2
3
4
5
6
7
8
9
1. Flight Test of Sensor
2. Analysis of Sensor Output
3. Design of Stall Deterrent System Model for Simulator
4. Stall Deterrent System Simulation
5. System Evaluation on NASA Langley General Aviation Aircraft Simulator
6. Analysis
7. Final Report
Original Proposal
Current Schedule 3/1/76

Table 2

Flight Test Stall Maneuvers

Maneuver	Flap Setting Degree	Power Setting	Sideslip Angle Degree	Remarks
0	0	Trim	0	60,70,80,90 mph constant speed segments for system calibration
1	0	Full	0	
2	0	Trim @ 70 mph	0	
3	0	Idle	0	
4	Full	Full	0	
5	Full	Trim @ 70 mph	0	
6	Full	Idle	0	
7	0	Trim @ 70 mph	10	Wings level sideslip
8	0	Trim @ 70 mph	20	
9	0	Trim @ 70 mph	-10	
10	0	Trim @ 70 mph	-20	
11	0	Trim @ 70 mph	10	Ailerons neutral
12	0	Trim @ 70 mph	-10	Ailerons neutral
13	Full	Trim @ 70 mph	10	Wings level sideslip
14	Full	Trim @ 70 mph	-10	
15	0	Full	0	60°left 2"g" accelerated stall
16	0	Full	0	60°right bank 2"g" accelerated stall
17	0	Landing & Takeoff		
18	1/2	Landing & Takeoff		
19	Full	Landing & Takeoff		

Table 3

Flight Test Log

Flight Number	Date	Purpose of Flight	Data Required	Crew	Remarks
1	12/15/75	System Checkout	No	Ebersole Bennett	α-β probe failure
2	12/15/75	System Checkout	Yes	Ebersole Bennett	Data measured, but temperature drift noted on position sensors
3	1/15/76	Airspeed Calibration and α Upwash Measurement	Yes	Ebersole Bennett	Quick check of systems
4	1/16/76	Airspeed Calibration	Yes	Ebersole Bennett	Check of temperature drift for position sensor outputs
5	1/19/76	Airspeed Calibration and α Upwash Calibration	No	Ebersole Bennett	Inclinometer sticking
6	1/27/76	Airspeed Calibration and α Upwash Calibration	Yes	Ebersole King	Finally made calibration
7	1/27/76	α-β System Check	No	Ebersole Bennett	β probe giving trouble
8	1/28/76	Stall Series Sensor 70% chord 68% span 1 1/4" h. 1/4"slot left, 1 1/2" h. hole right	No	Ebersole Bennett	Recorder failed after 3 maneuvers

9	2/5/76	Repeat of Flight 8	No	Ebersole Bennett	Voice track not recorded
10	2/9/76	Sensor position of Flight 8 1 1/4" h. hole left, 1" h. hole right	Yes	Ebersole King	Finally good data
11	2/12/76	Sensor position of Flight 8 1 1/4" h. 1/4" slot left 1 1/2" h. hole right	No	Ebersole King	α probe sticking
12	2/17/76	Sensor position of Flight 8 1 1/2" h. hole both left and right	Yes	Ebersole Bennett	Flight record to allow study of summing both sensor outputs for control
13	2/20/76	Sensor position of Flight 8 1 3/4" h. hole left, 1 1/4" h. 1/4" slot right	Yes	Ebersole Bennett	
14	2/22/76	Sensor position of Flight 8 2" h. hole left, 1 1/2" h. 1/2" slot right	Yes	Ebersole Bennett	Discovered static line off transducer
15	2/25/76	Photo record of wing stall patterns	Yes	Ebersole Bennett	Used Cessna 150 for chase. Made all possible maneuvers. Yaw right only
16	2/27/76	Sensor at 60% chord 68% span 1 1/2" h. hole left, 1" h. hole right	Yes	Ebersole King	Moved sensors forward for less yaw dependence
17	3/1/76	Sensor position of Flight 16 1 3/4" h. hole left, 1 1/4" h. hole right	Yes	Ebersole King	

Figure 1. Cessna 319 used for Stall Deterrent Study

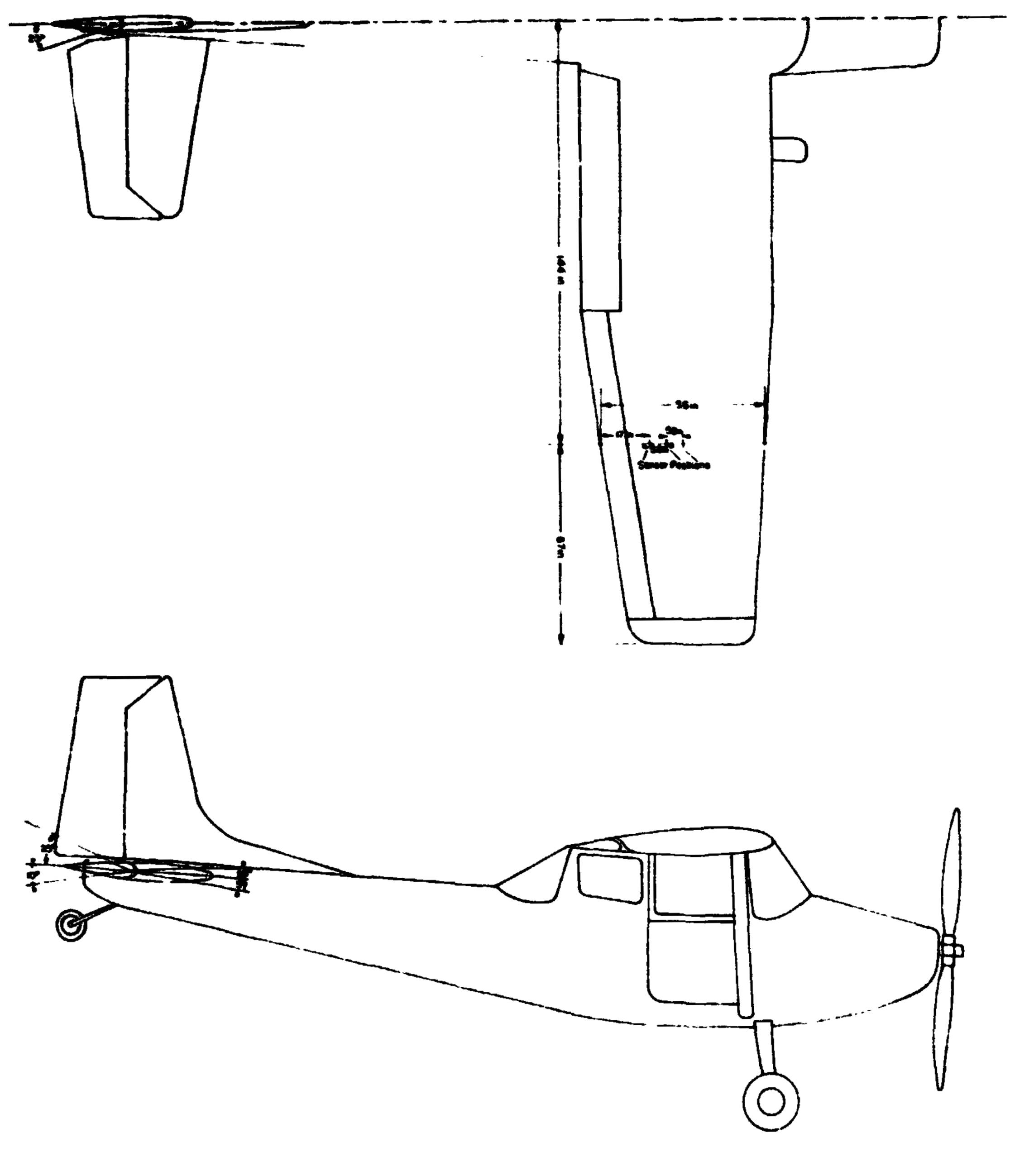

Fig. 2 3-view of Cessna 319 with Sensor ~c Positions

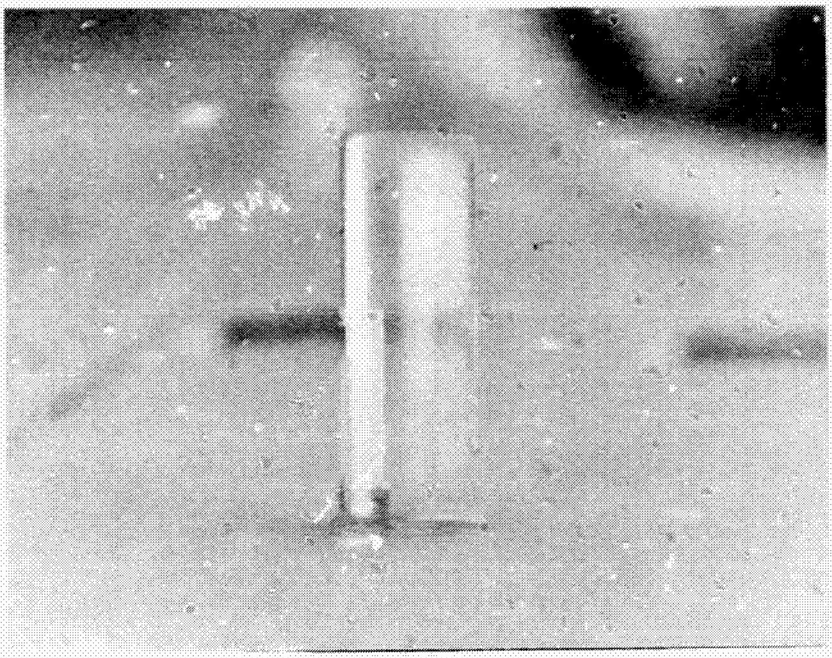

a. Slot Orifice

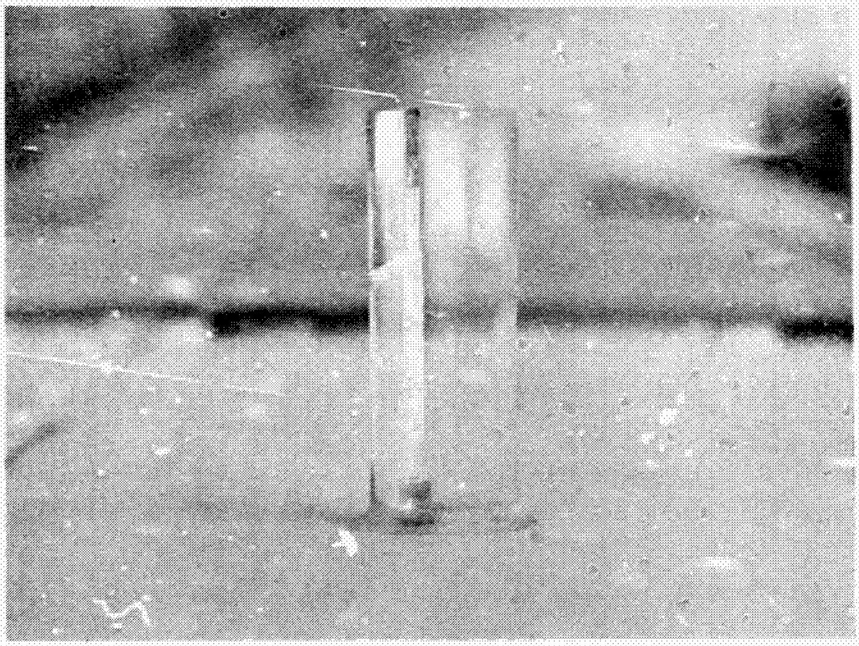

b. Hole Orifice

Figure 3. Hole and Slot Orifice Acoustic Sensors

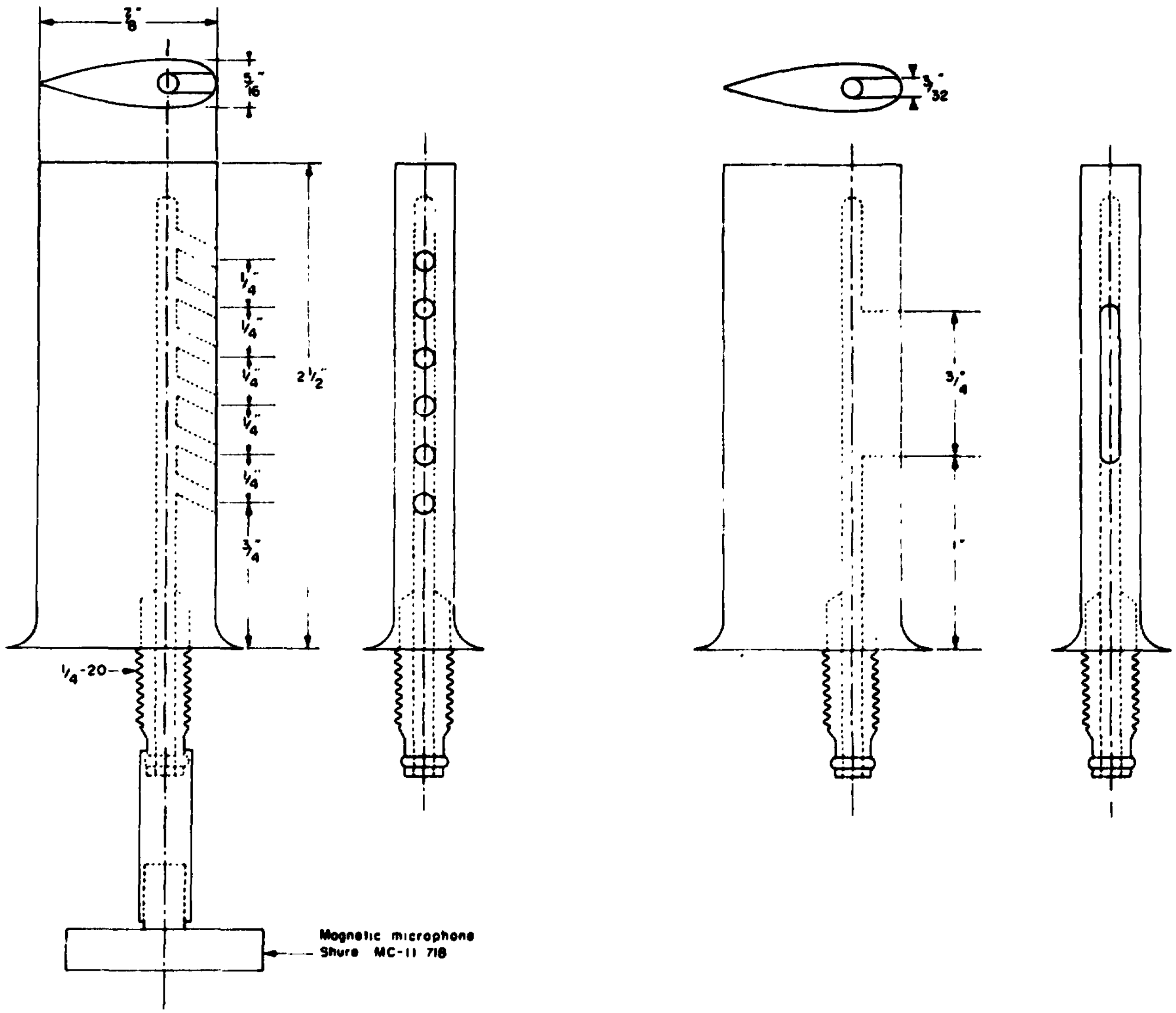

Fig. 4 Sensor Configurations used for Study

ORIGINAL PAGE IS
OF POOR QUALITY

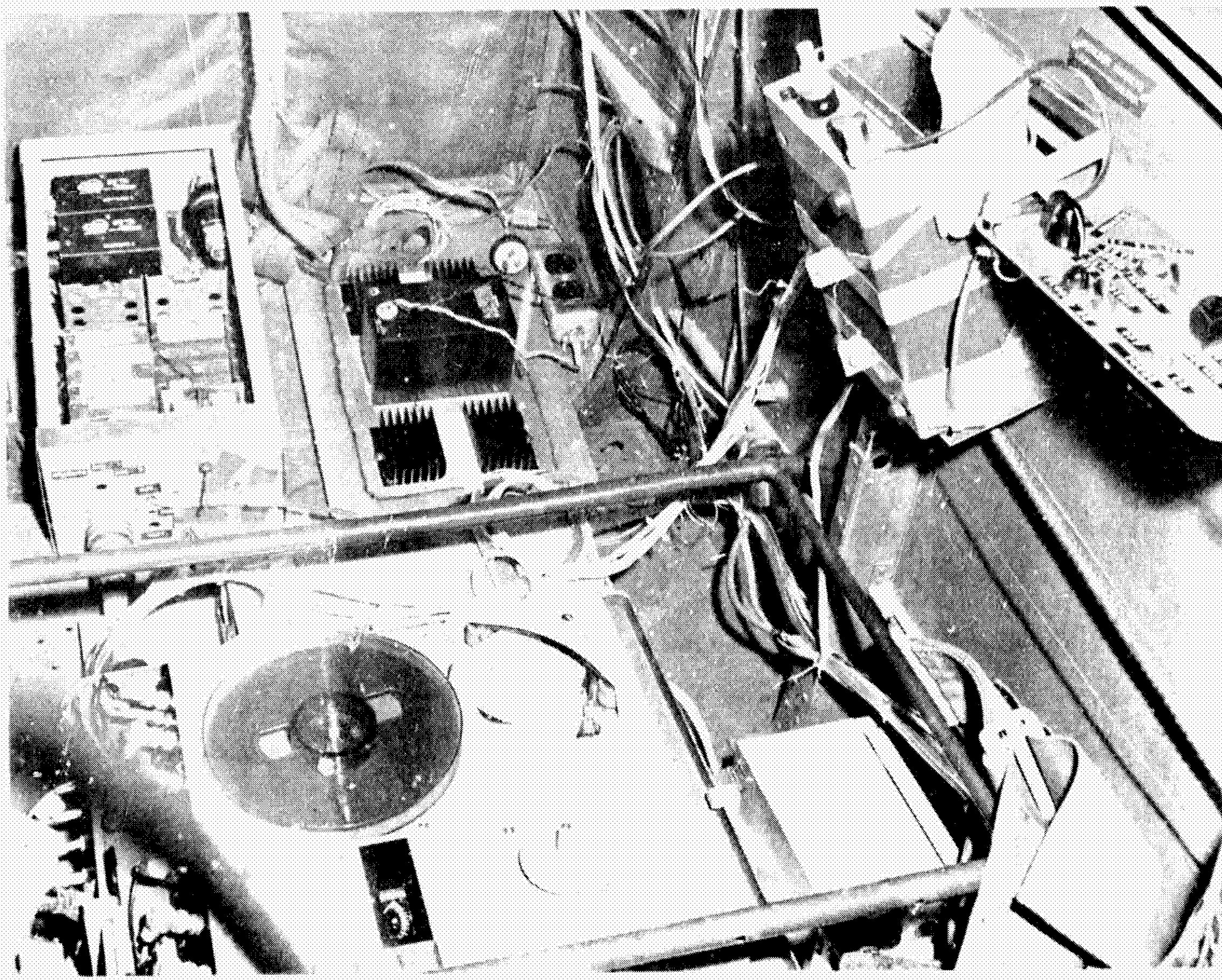

Figure 5. Instrumentation Installation in Cessna 319

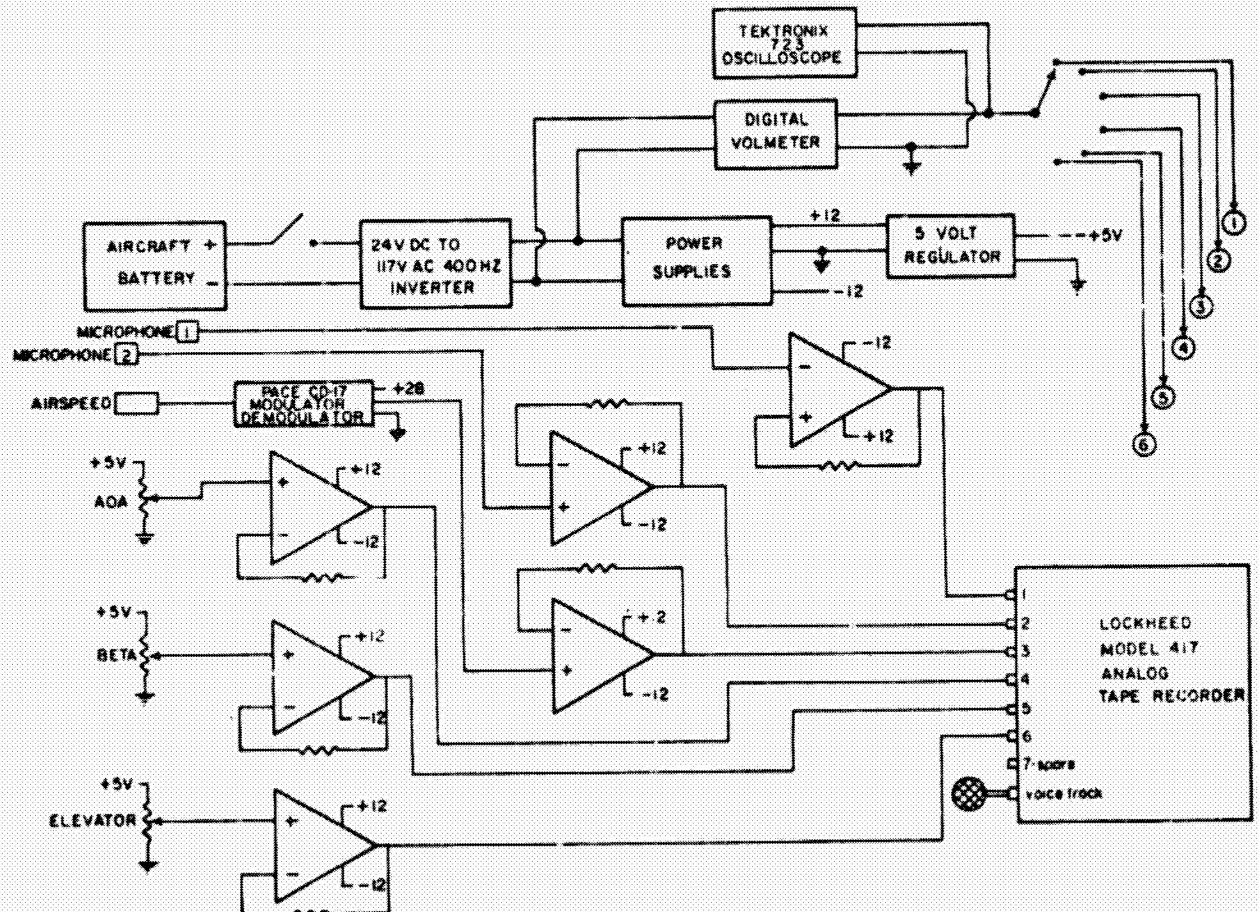

STAL DETERRENT INSTRUMENTATION SYSTEM

BLOCK DIAGRAM

Fig. 6 Schematic of Instrumentation System Installed in Cessna 319

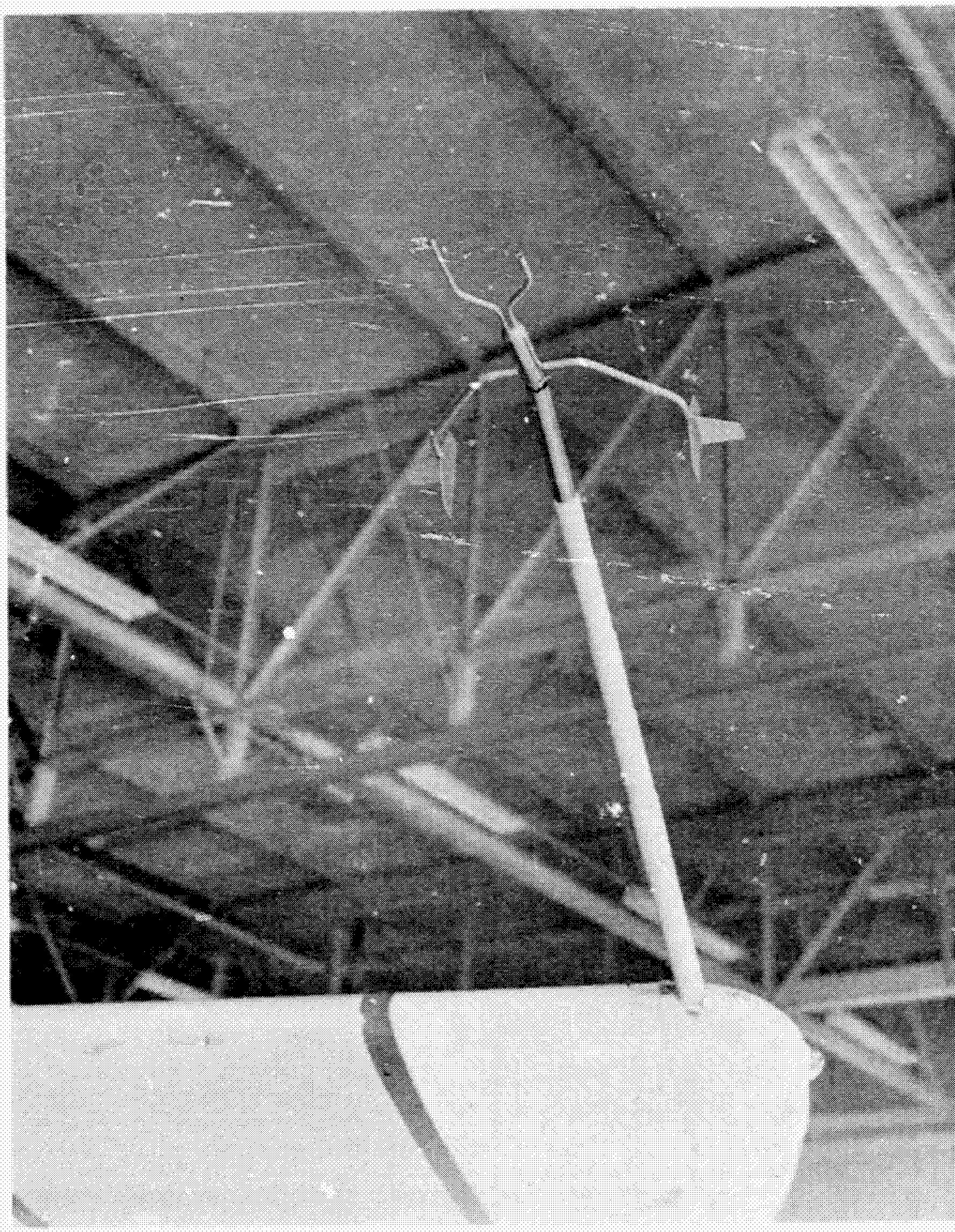

Figure 7. Alpha - Beta - Airspeed Probe

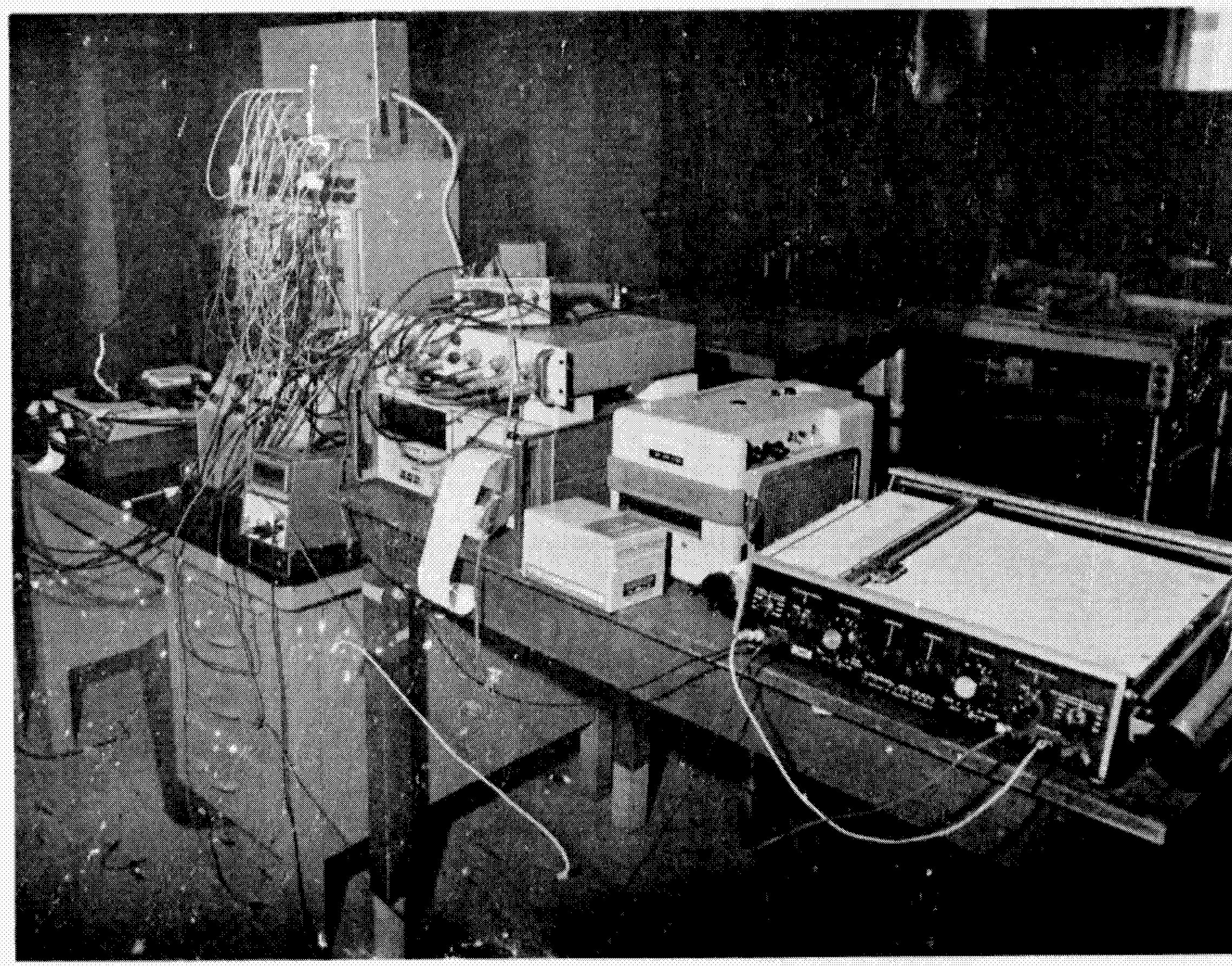

Figure 8. Analog Data Reduction System

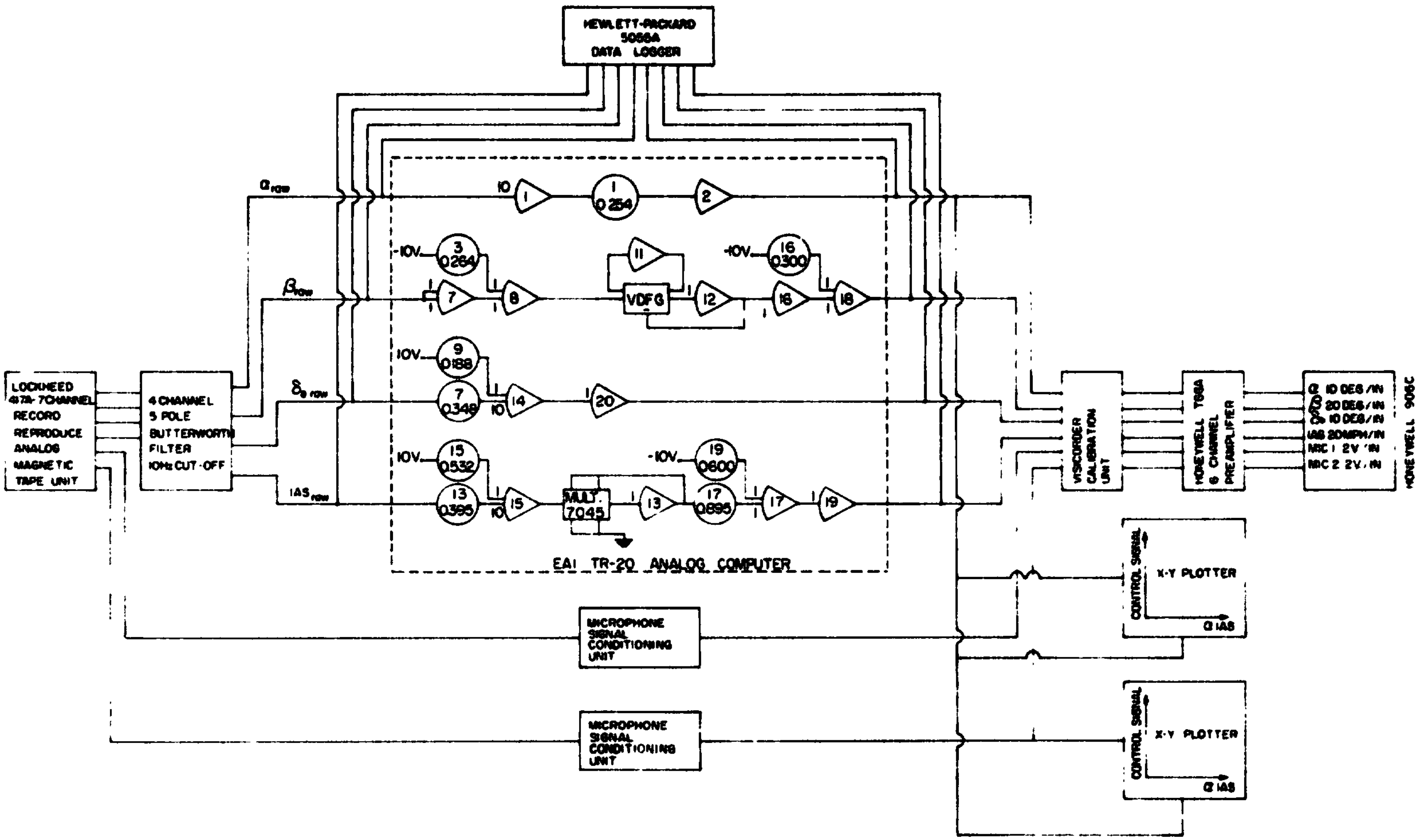

Fig. 9 Schematic of Data Reduction System

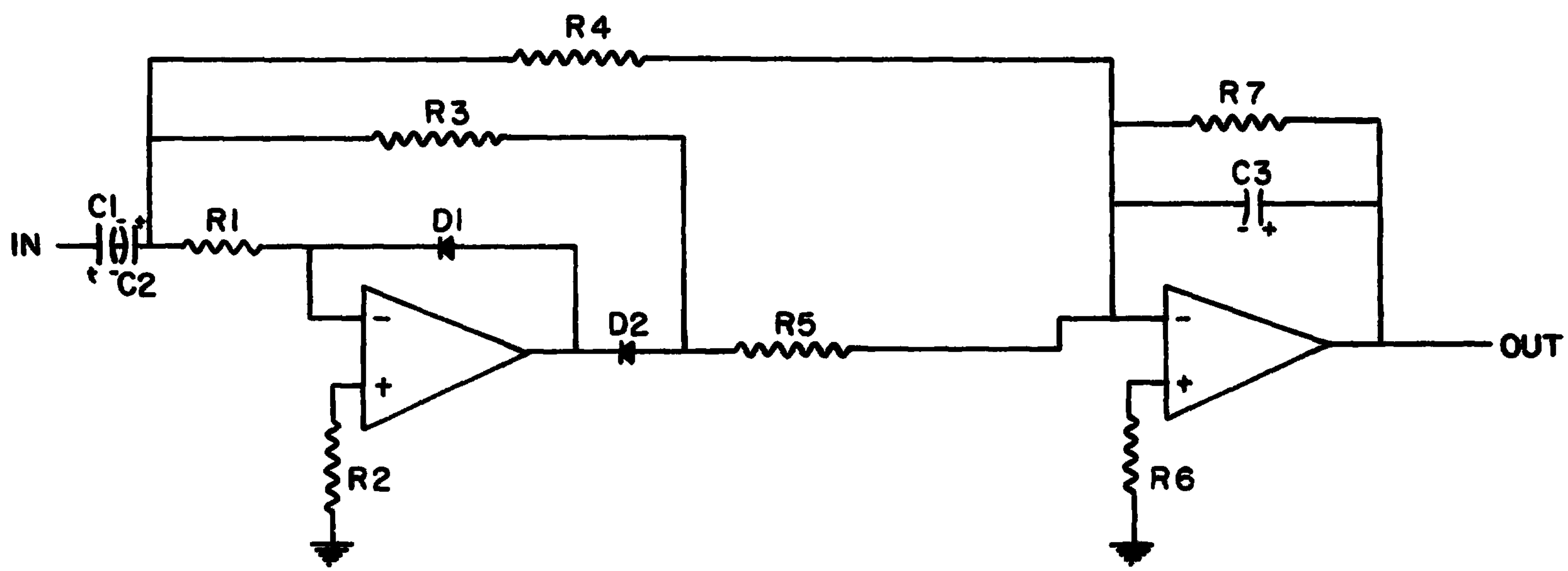

Fig. 10 Sensor Acoustic Output Signal Conditioning Circuit

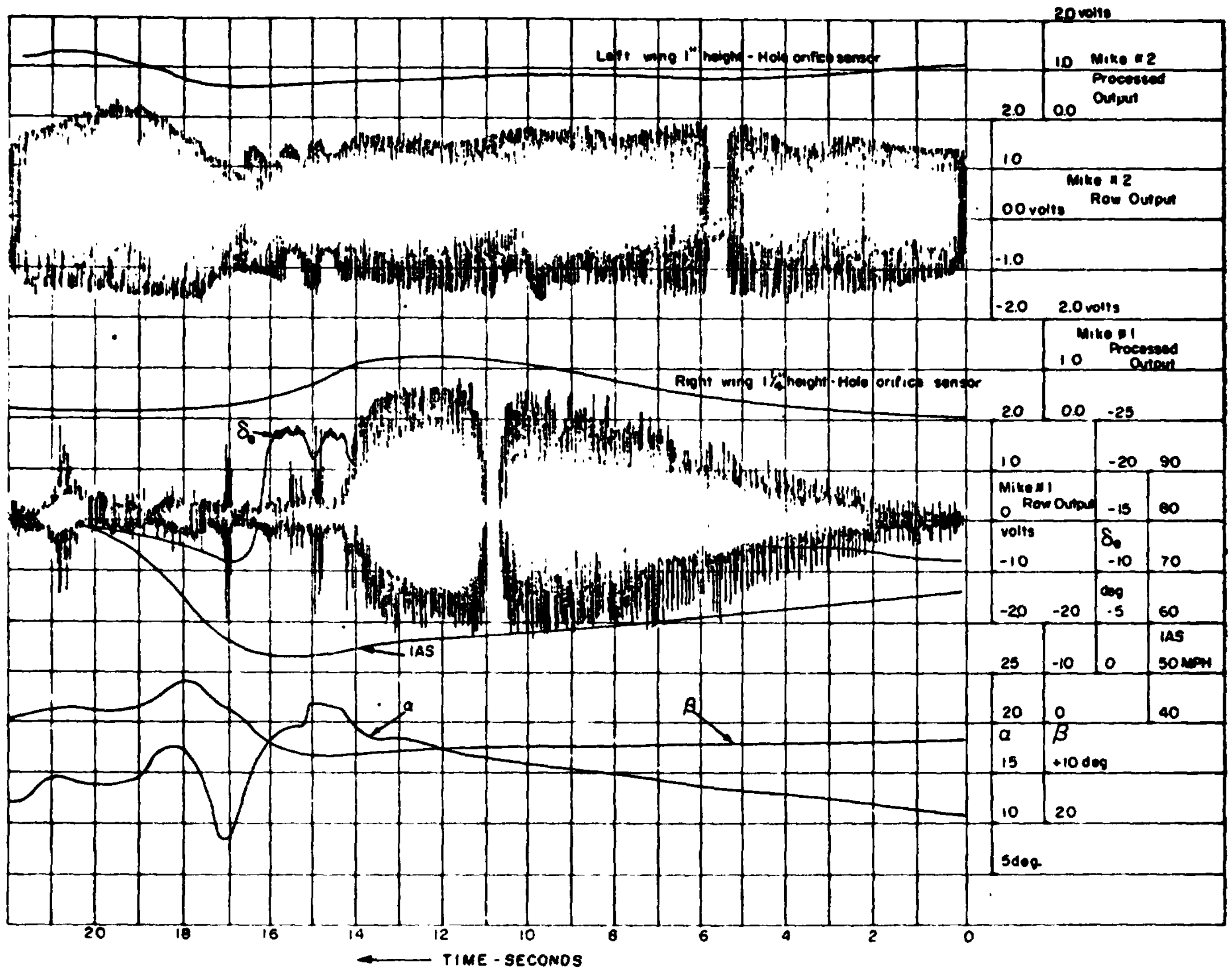

Fig. 11 Sensor Outputs Versus Time for Stall Maneuver with 70 MPH Trim Power, 0 Degree Flap and 0 Degree Sideslip Angle

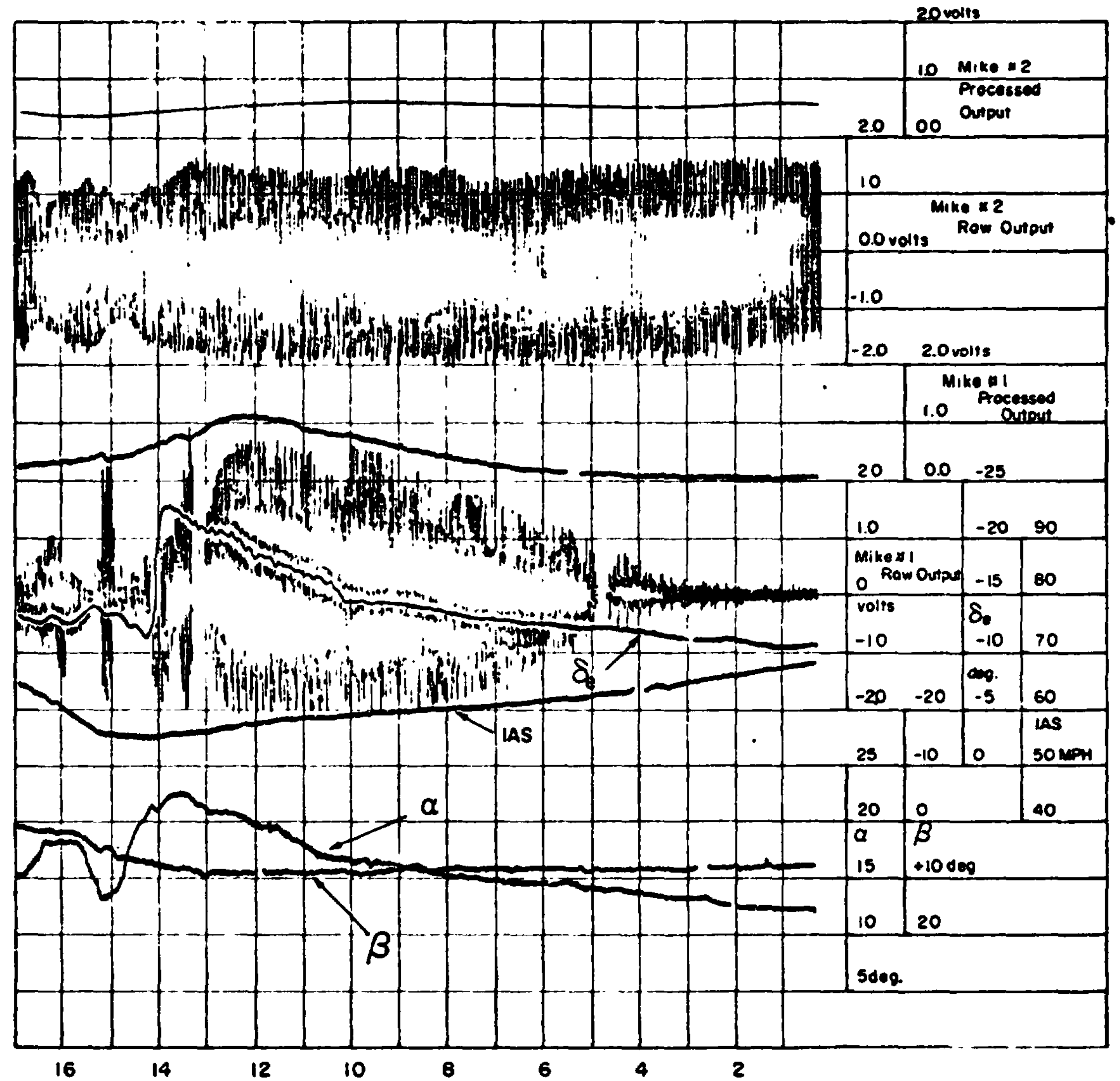

Fig. 17. Sensor Outputs Versus Time for Stall Maneuver with 70 MPH Trim Power, 0 Degree Flap and 10 Degree Sideslip Angle

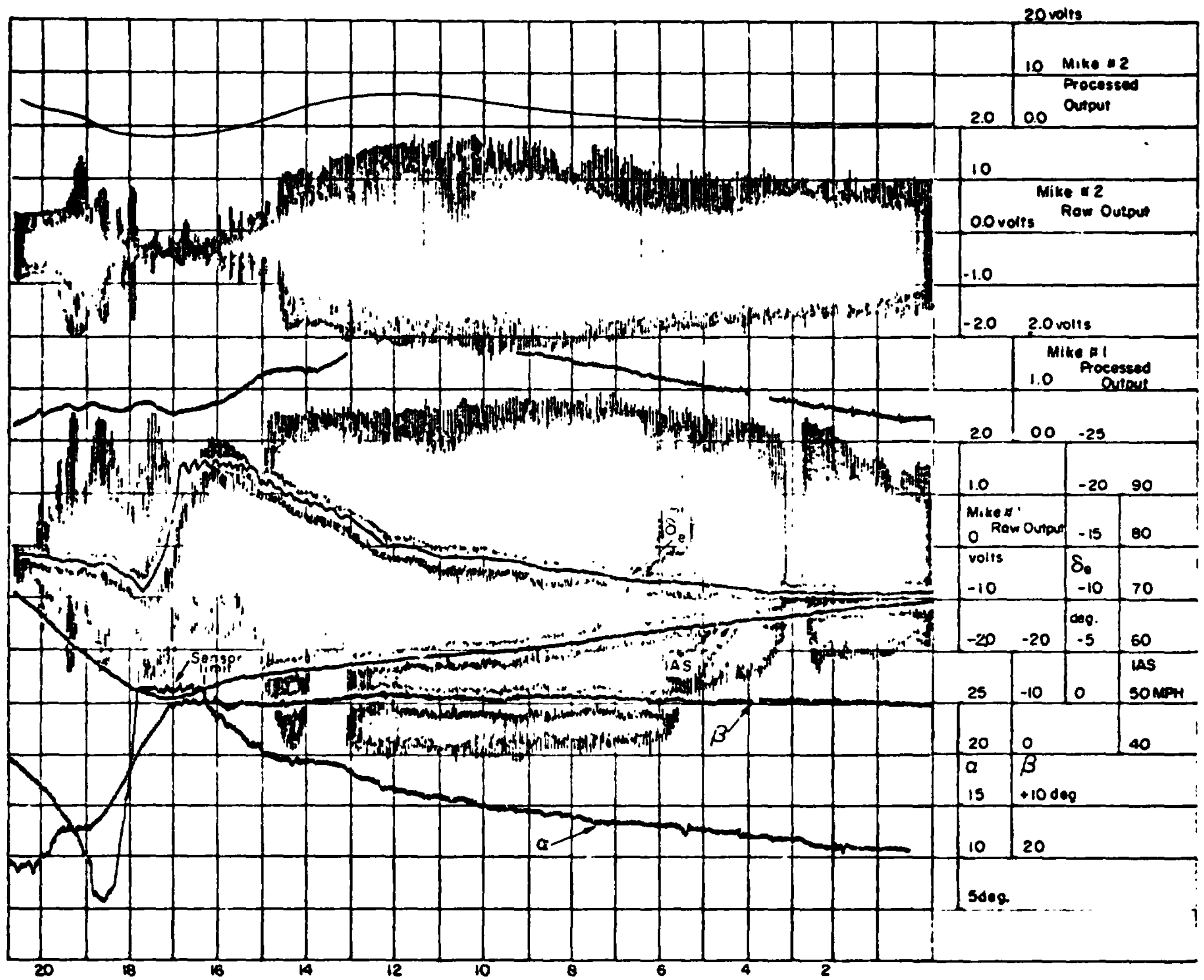

Fig. 13. Sensor Outputs Versus Time for Stall Maneuver with 70 MPH Trim Power, 0 Degree Flap and -10 Degree Sideslip Angle

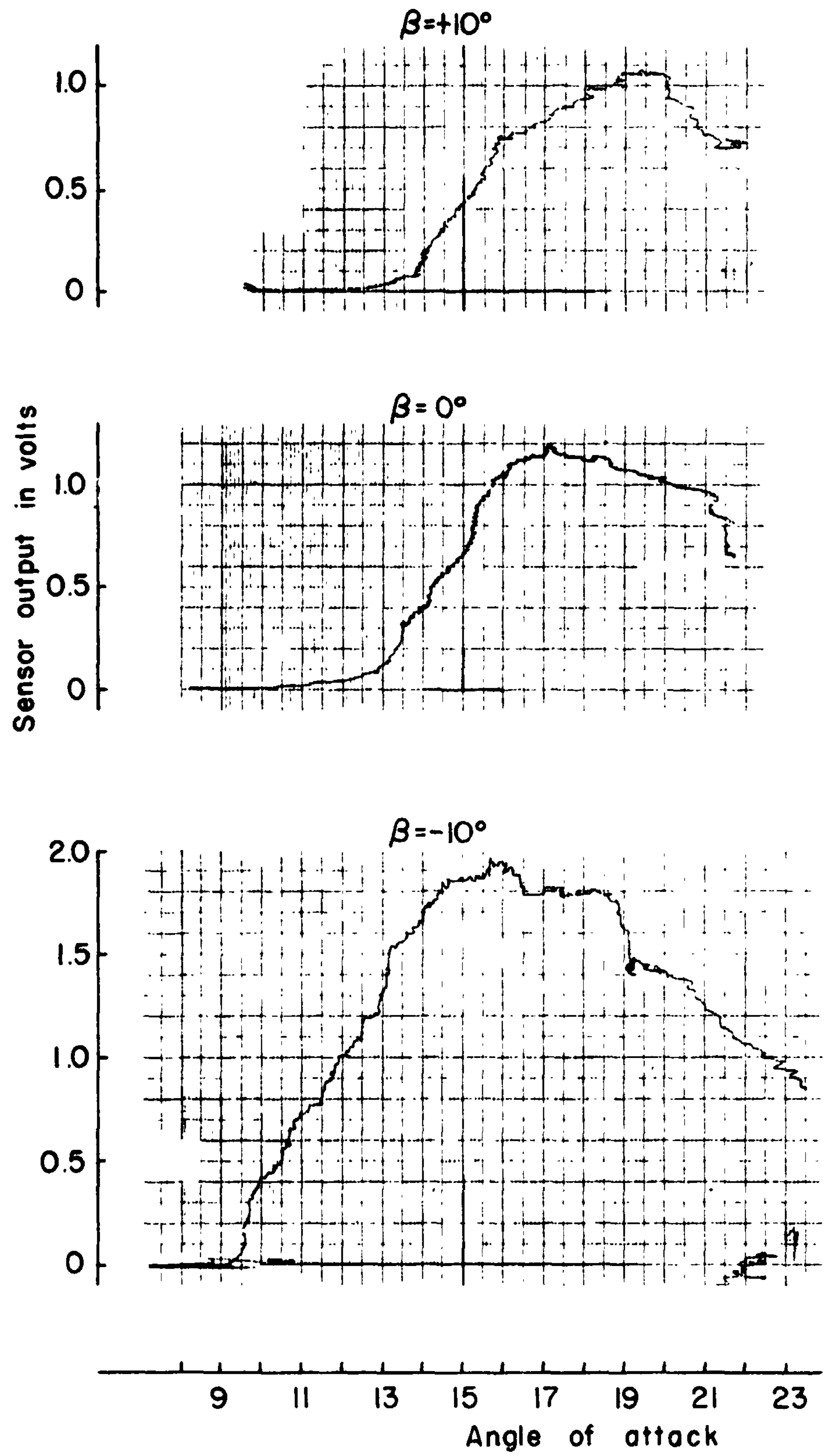

Fig. 14. Processed Acoustic Signal Versus Angle of Attack for 1 1/4" Height Round Orifice Mounted on Right Wing for 0 and ±10 Degree Sideslip Angles. Trim at 70 MPH Power Setting and 0 Degree Flap

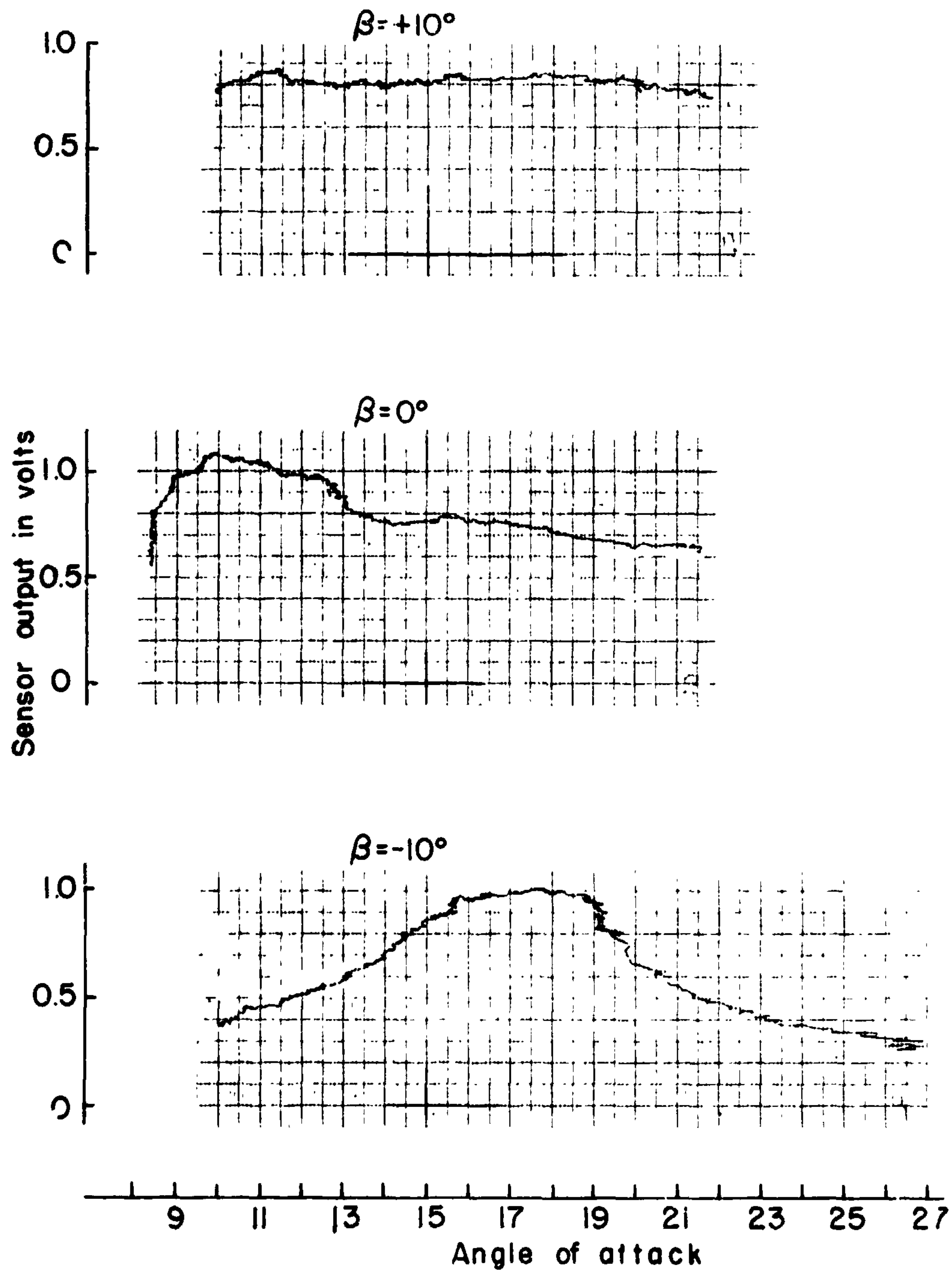

Fig. 15. Processed Acoustic Signal Versus Angle of Attack for 1" Height Round Orifice Mounted on Left Wing for 0 and ±10 Degree Sideslip Angles. Trim at 70 MPH Power Setting and 0 Degree Flap

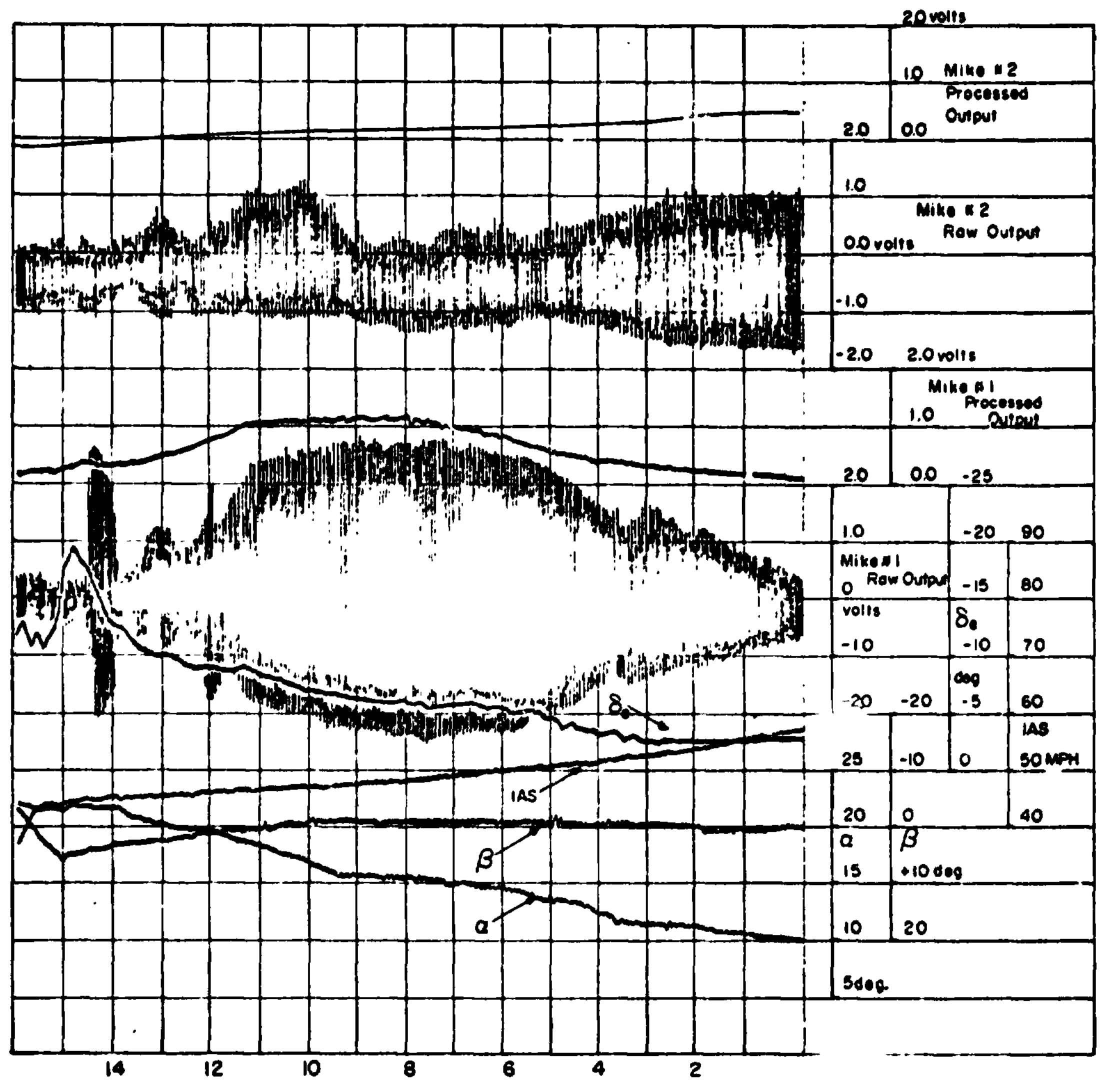

Fig. 16. Sensor Outputs Versus Time for Stall Maneuver with 70 MPH Trim Power, Full Flap and 0 Degree Sideslip Angle

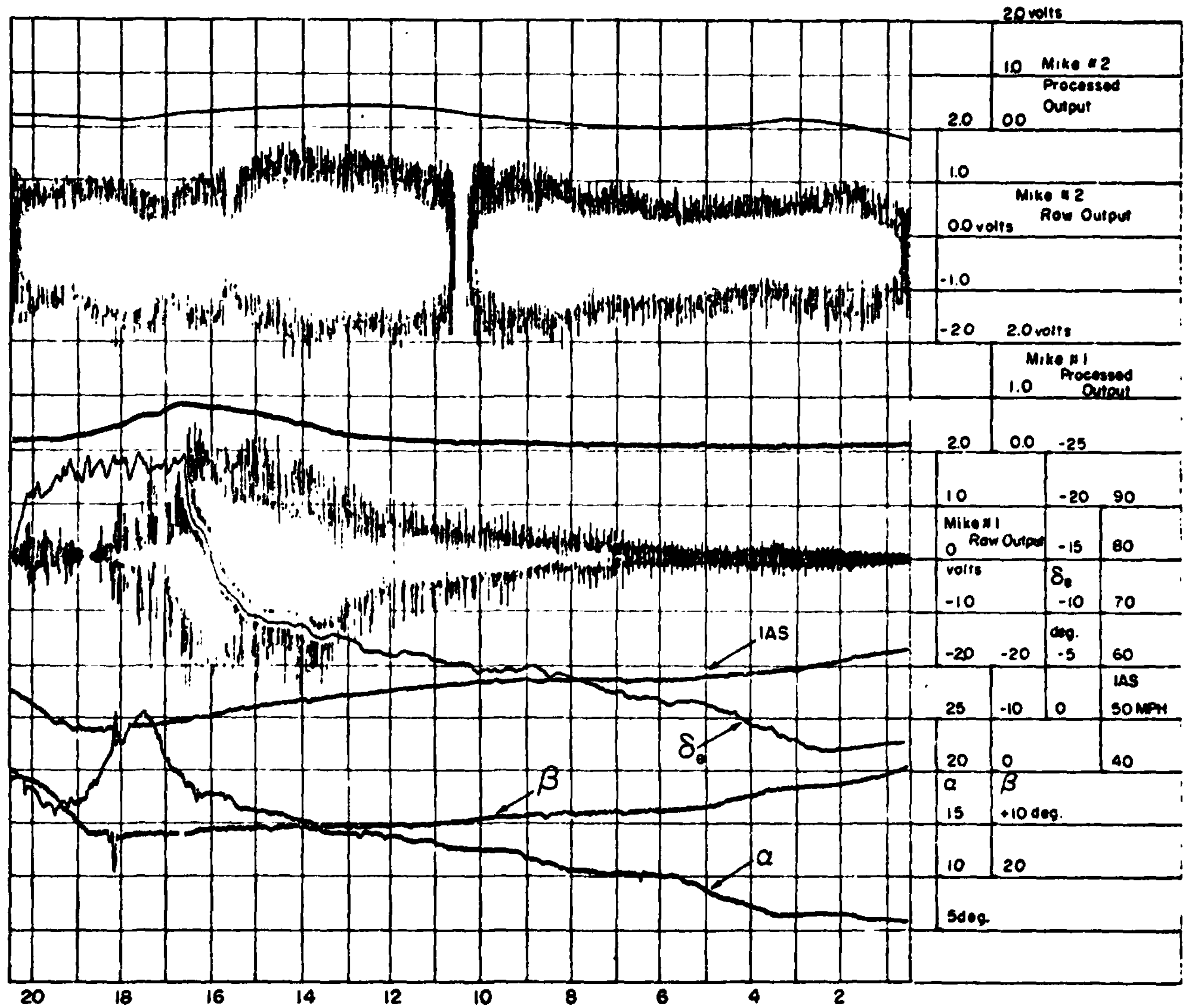

Fig. 17 Sensor Outputs Versus Time for Stall Maneuver with 70 MPH Trim Power, Full Flap and 0 Degree Sideslip Angle

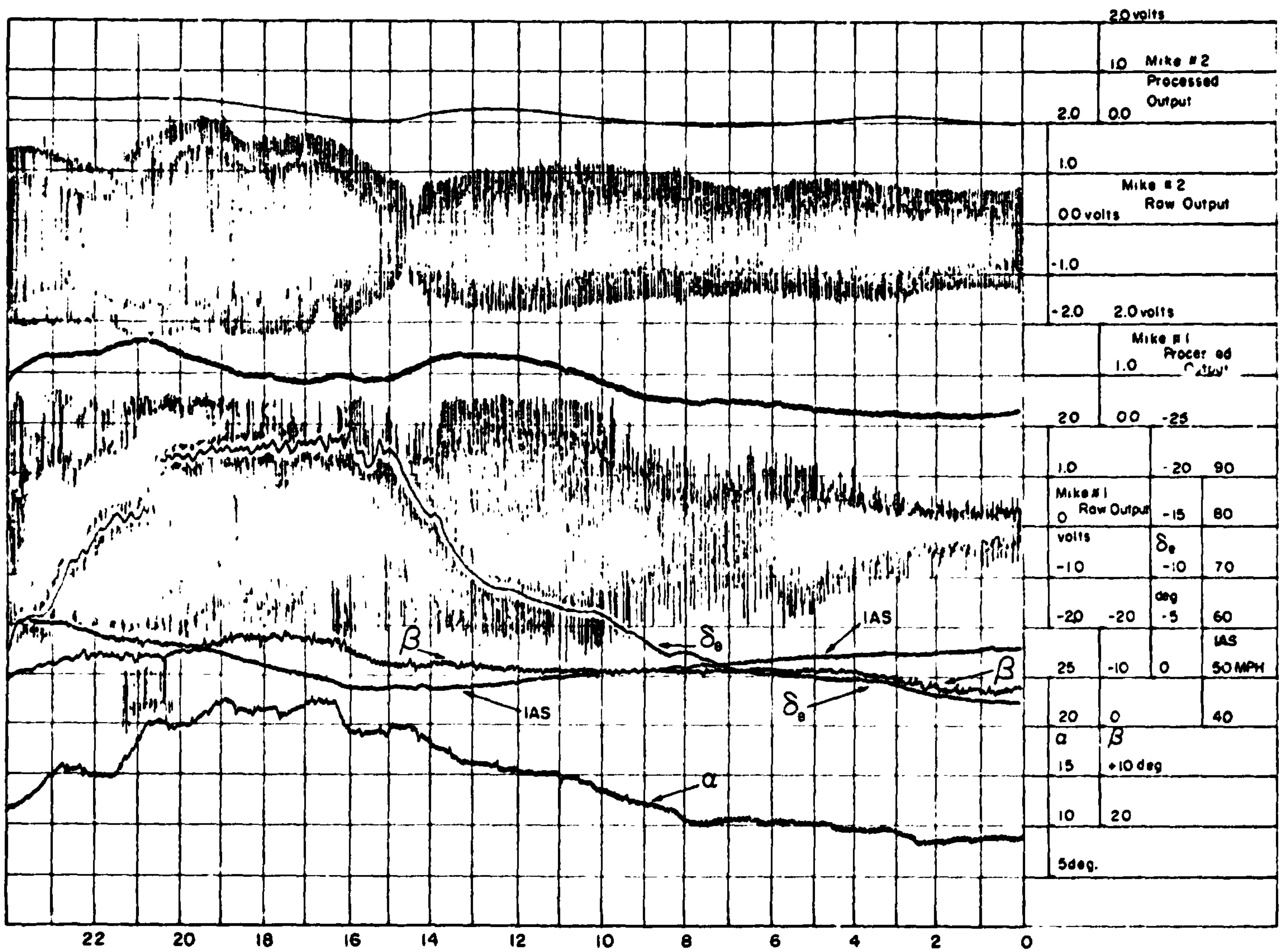

Fig. 18 Sensor Outputs Versus Time for Stall Maneuver with 70 MPH Trim Power, Full Flap and -10 Degree Sideslip Angle

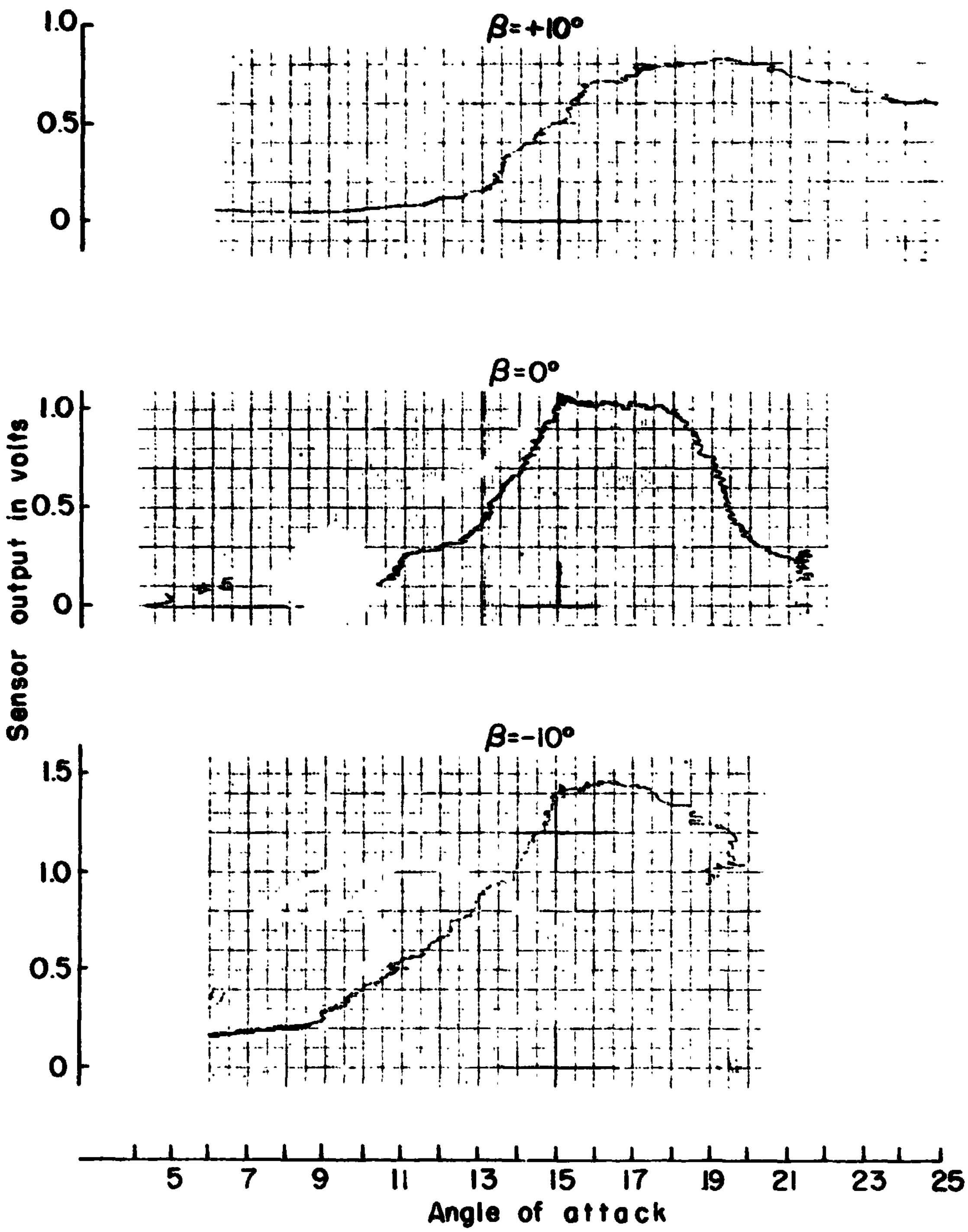

Fig. 19 Processed Acoustic Signal Versus Angle of Attack for 1 1/4" Height Round Orifice Mounted on Right Wing for 0 and ±10 Degree Sideslip Angles. Trim at 70 MPH Power Setting and Full Flap

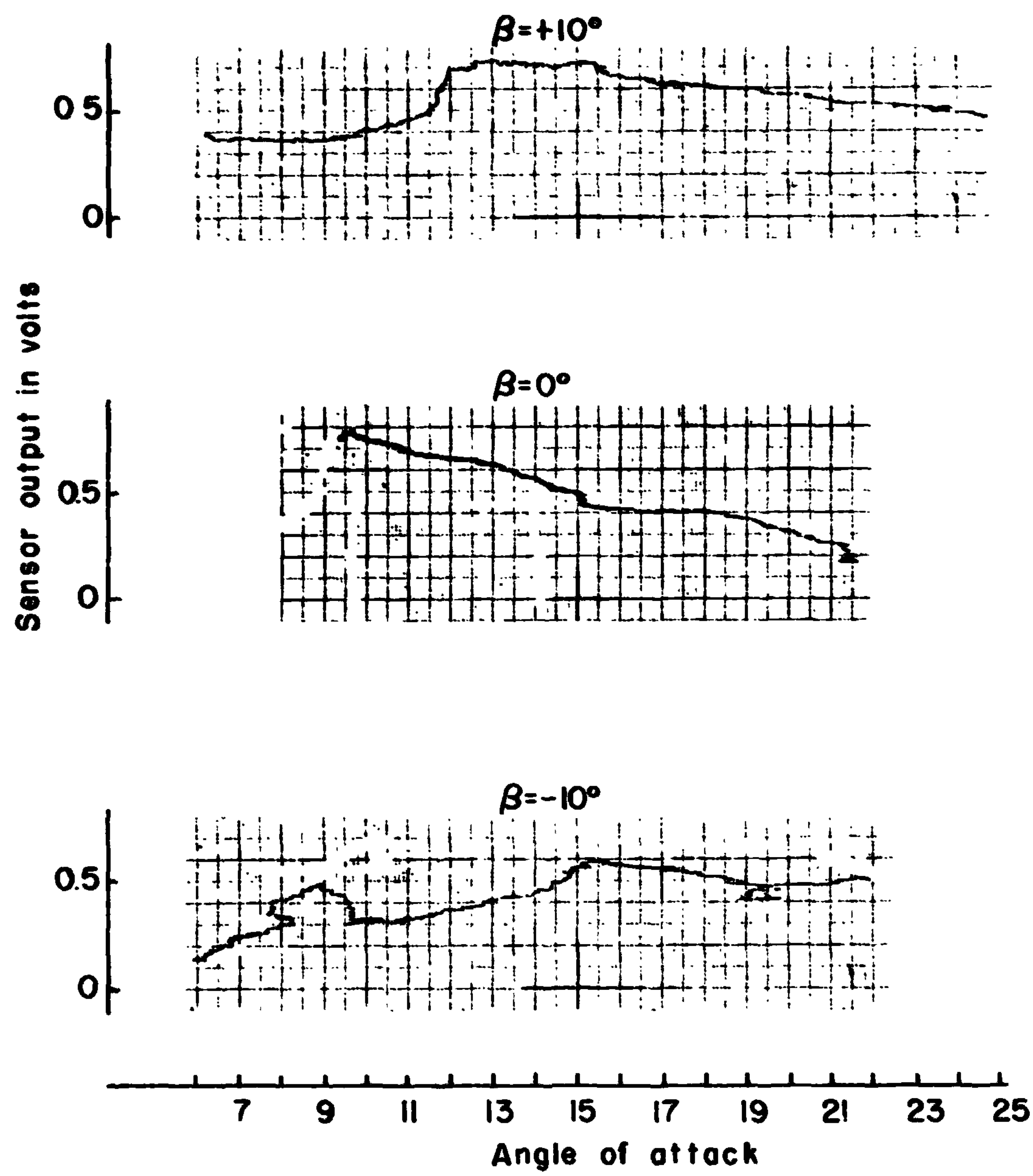

Fig. 20. Processed Acoustic Signal Versus Angle of Attack for 1" Height Round Orifice Mounted on Left Wing for 0 and ±10 Degree Sideslip Angles and Full Flap

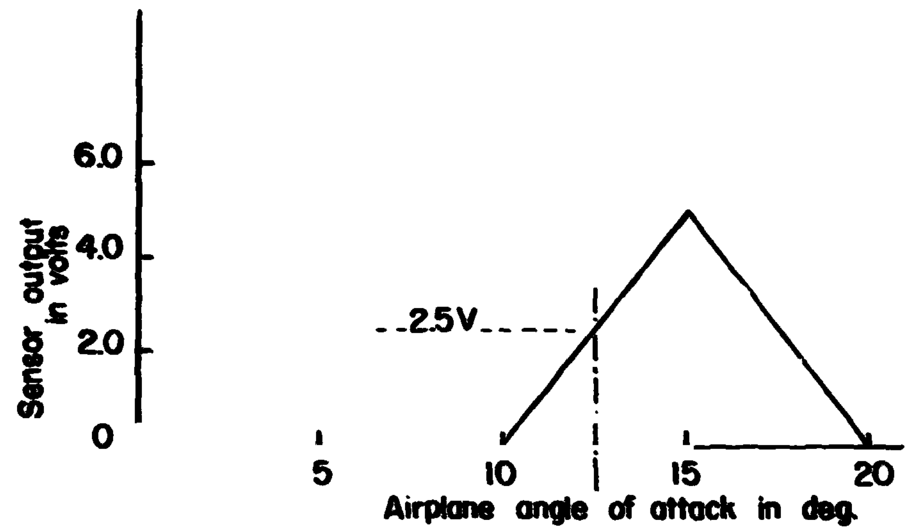

Fig. 21. Assumed Acoustic Sensor Processed Signal Output Versus Airplane Angle of Attack

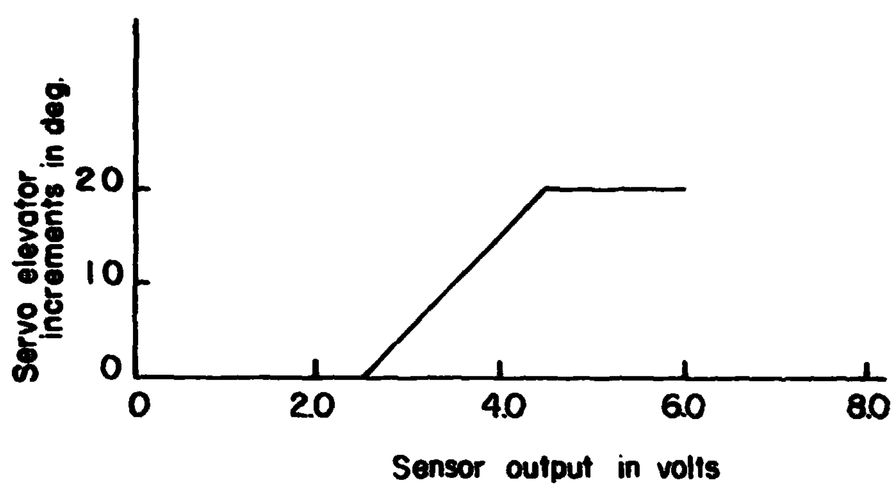

Fig. 22. Stall Deterrent System Elevator Increment Versus Error Voltage

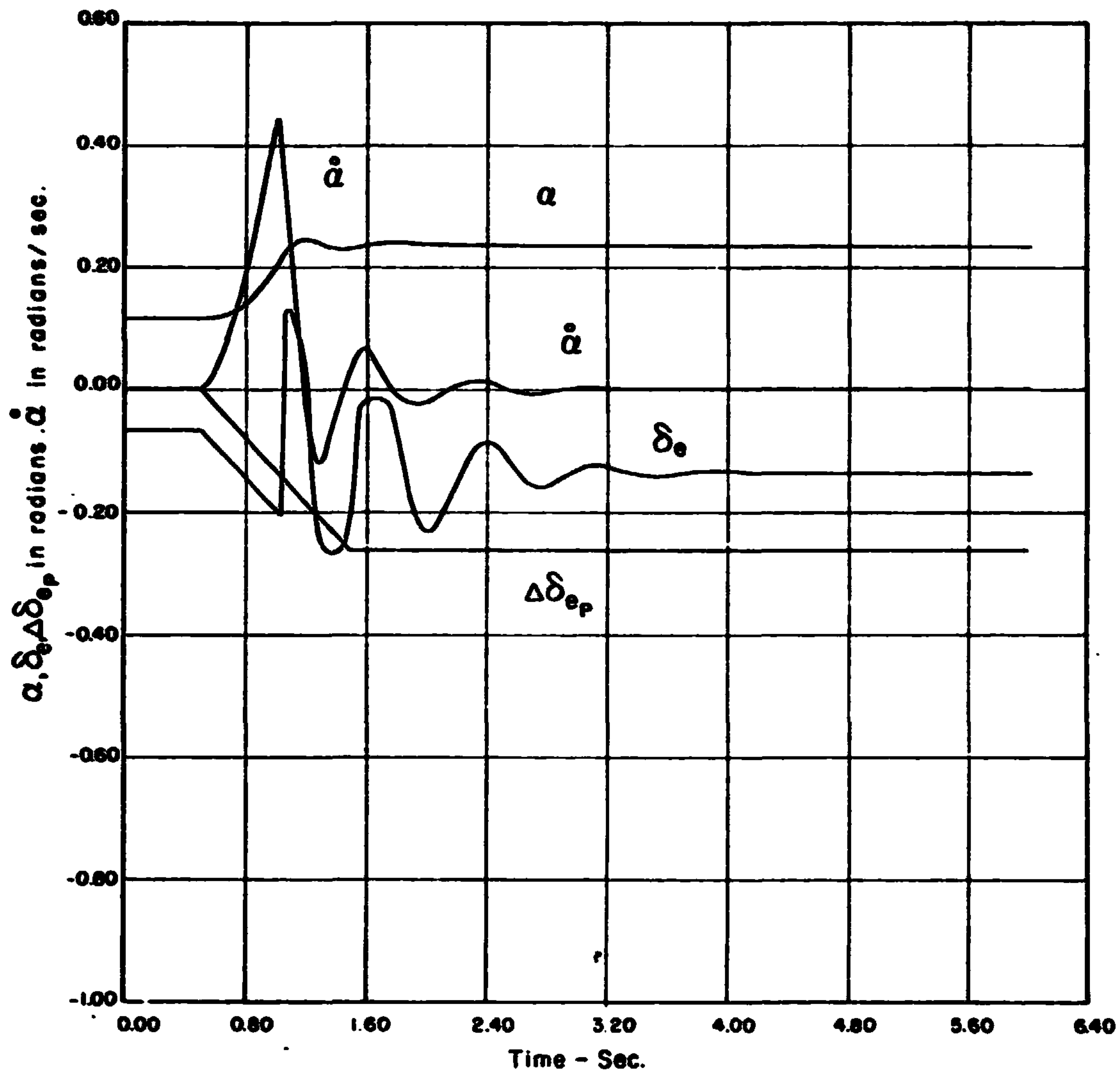

Fig. 23. Response of Stall Deterrent System to a 20 degree/sec Ramp Pilot Elevator Command Using a One Degree of Freedom Model

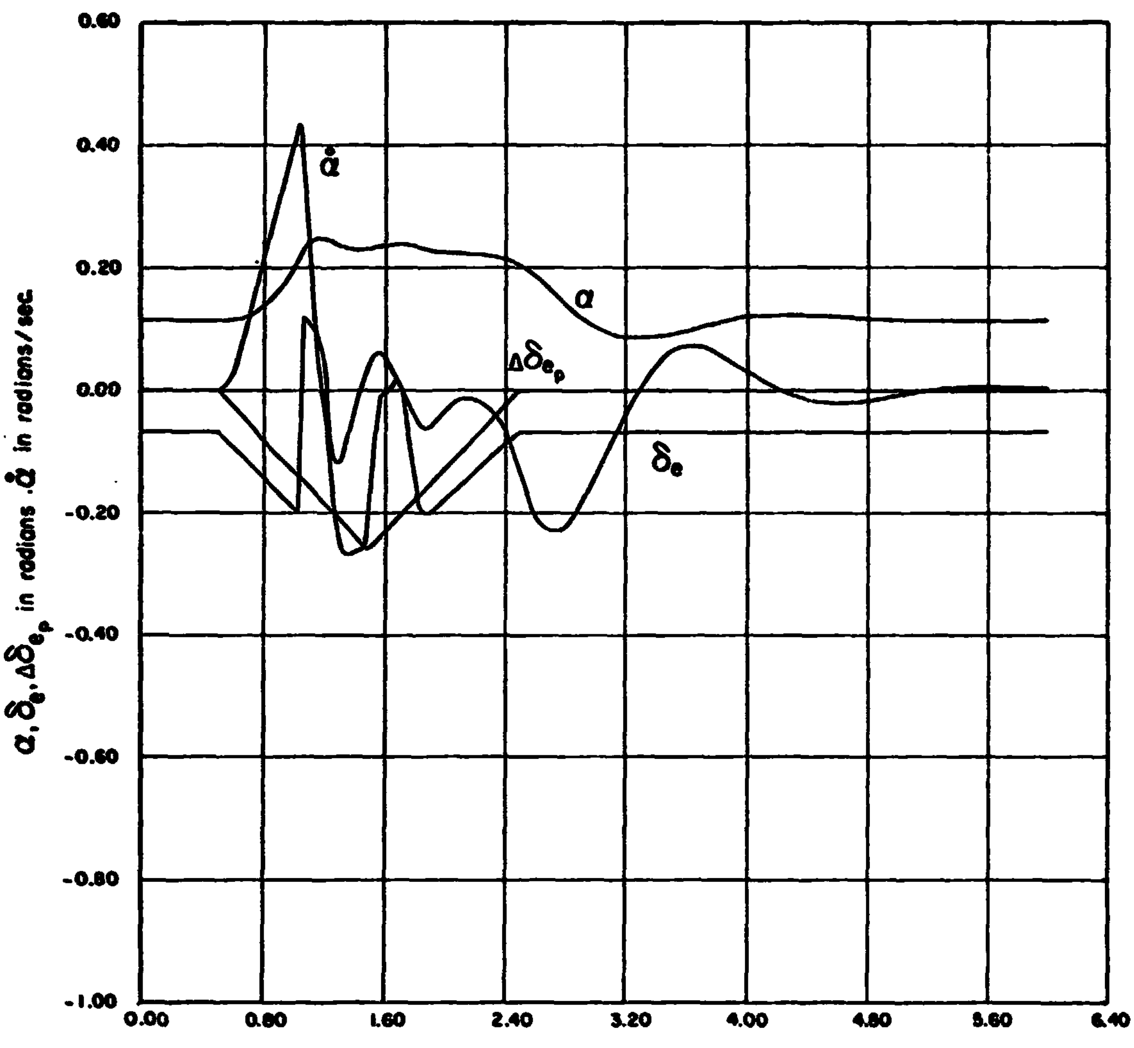

Fig. 24 Response of Stall Deterrent System to a 20 degree/sec. Spike Pilot Elevator Command Using a One Degree of Freedom Model